

Nonparametric inference for continuous-time event counting and link-based dynamic network models

Alexander Kreiß
Heidelberg University
Institute for Applied Mathematics
Im Neuenheimer Feld 205
69120 Heidelberg
Germany
kreiss@uni-heidelberg.de

Enno Mammen
Heidelberg University
Institute for Applied Mathematics
Im Neuenheimer Feld 205
69120 Heidelberg
Germany
mammen@math.uni-heidelberg.de

Wolfgang Polonik
Department of Statistics
University of California, Davis
One Shields Ave.
Davis, CA 95616
USA
wpolonik@ucdavis.edu

July 21, 2022

Abstract

A flexible approach for modeling both dynamic event counting and dynamic link-based networks based on counting processes is proposed, and estimation in these models is studied. We consider nonparametric likelihood based estimation of parameter functions via kernel smoothing. The asymptotic behavior of these estimators is rigorously analyzed by allowing the number of nodes to tend to infinity. The finite sample performance of the estimators is illustrated through an empirical analysis of bike share data.

1 Introduction

This work is studying a flexible modeling approach that is useful for both modeling dynamic interactions as well as dynamic networks in continuous time. These two notions, while related, are somewhat different. Interactions are instantaneous events between two nodes, a sender and a receiver. For instance, one person sending an e-mail to another person, is an example for an interaction event, and the popular Enron e-mail data is based on such events. While such interactions can be thought of as edges between two nodes, and while these nodes persist over time, each such edge only exist for an infinitesimal time. Persisting edges can be built by aggregating the interactions over a certain time period. This is not to say that persisting networks cannot change over time. Edges and nodes can be added or deleted over time, but we think of edges in a networks as having a certain positive lifespan.

Random networks/graphs have been considered in various scientific branches since a long time, in particular in the social sciences (c.f. the textbook by Wasserman and Faust, 1995). The importance of the analysis of random networks within the more statistical and machine learning literature is more recent, but corresponding literature is significant by now (e.g. see Kolaczyk, 2009 or Goldenberg et al. 2010). The reason for this increase in significance is not least due to the development of modern technologies that lead to the ever increasing number of complex data sets that are encoding relational structures. Examples for real network data can be found at the Koblenz Network Collection KONECT, the European network data collection SocioPatterns, the MIT based collection Reality Commons, the data sets made available by the Max Planck Institute for Softwaresysteme (MPI-SWS), or the Stanford Large Network Dataset Collection (SNAP). In this paper, we will use the Capital Bikeshare Performance Data (see <http://www.capitalbikeshare.com/system-data>), which is a data set collected on the Washington, DC bikeshare system.

Modeling and analyzing dynamic random networks is challenging as networks can have a multitude of different topological properties. Such topological properties are measured by various quantities, including the flow through the network, the degree distribution, centrality, the existence of hubs, sparsity etc. Time-varying or dynamic random networks appear quite naturally, even though the dynamic aspect significantly adds to the complexity of modeling and analyzing the networks. Early work on networks involving temporal structures can already be found in Katz and Proctor (1959), who consider a discrete time Markov process for friendships (links). Other relevant literature using discrete time settings include work on dynamic exponential random graph models (Sarkar and Moore, 2006, Sarkar et al., 2007, Guo et al., 2007, Ahmed and Xing, 2009, Hanneke, Fu and Xing, 2010, Krivitsky, 2012, Krivitzky and Handcock, 2014), dynamic infinite relational models (Ishiguro et al. 2010), dynamic block models (Ho et al. 2011, Xing et al., 2014, Xu and Hero, 2014, Xu, 2015), dynamic nodal states models (Kolar and Xing, 2009, Kolar et al., 2010), various dynamic latent features model (Foulds et al, 2011), dynamic multi-group membership models (Kim and Leskovec, 2013), dynamic latent space models (Durante and Dunsen, 2014,

Sewell and Chen, 2015), and dynamic Gaussian graphical models (Zhou et al, 2008, Kolar and Xing, 2012). Also time-continuous models have been discussed in the literature. They include link-based continuous-time Markov processes (Wassermann, 1980, Leenders, 1995, Lee and Priebe, 2011), actor-based continuous-time Markov processes (Snijders, 1996, 2001, Snijders et al. 2010), and also models based on counting processes as in Perry and Wolfe (2013) (who are considering the modeling of interaction data). Link Prediction, a problem related to the analysis of dynamic networks, received quite some attention in the computer science literature (e.g. see Liben-Nowell and Kleinberg, 2007, or Backstrom and Leskovec, 2011).

Despite the strong interest in dynamic models for networks, rigorous statistical analysis of corresponding estimators (asymptotic distribution theory) are relatively sparse, in particular in the case of time-varying parameters, as considered here. The temporal models in the literature are usually Markovian in nature. In contrast to that our continuous-time model based on counting processes allows for non-Markovian structures (i.e. dependence on the infinite past). This increases flexibility in the modeling of the temporal dynamics. Our model also allows for a change of the network size over time without the network degenerate in the limit. Moreover, we are presenting a rigorous analysis of distributional asymptotic properties of the corresponding maximum likelihood estimators. To the best of our knowledge, no such analysis can be found in the literature, even for the simpler models indicated above.

In section 2, we introduce our model (section 2.1), define our likelihood-based estimators, and present our main result on the pointwise asymptotic normality of our estimators in section 2.2. In section 3, we demonstrate the flexibility of our approach by presenting an analysis of the Capital Bikeshare Data. The proof of our main result is deferred to Section 4.

2 Link-based dynamic models

2.1 Link-based dynamic models with constant parameters

In this section, we will discuss models where the parameters are fixed. In the rest of the paper we will generalize this class of models to specifications where the parameters are allowed to depend on time. For fixed parameters we have the following general model for interaction based observations. Let $V = \{1, \dots, n\}$ label the nodes of the network (in the literature also called actors or agents), and let $L_n = \{(i, j) : i < j, i, j \in V\}$ denote the set of all possible links (or edges) in a network, formed between the nodes V . For each pair of actors (i, j) we denote by $N_{n,ij}(t)$ the number of interactions between these two

$$N_{n,ij}(t) = \#\{\text{interaction events between } i \text{ and } j \text{ before or at time } t\}.$$

All results are formulated for undirected interactions, i.e., we assume that $N_{n,ij} = N_{n,ji}$ for all pairs (i, j) . This assumption is made for simplicity. All results can be formulated for the directed case as well (see also discussion given below, right after assumption (A1)). We assume that for $(i, j) \in L_n$, the processes $N_{n,ij}$ are one-dimensional counting processes with respect to an increasing, right continuous, complete filtration \mathcal{F}_t , $t \in [0, T]$, i.e. the filtration obeys the *conditions habituelles*, see Andersen et al. (1993), pp. 60. The σ -field \mathcal{F}_t contains all information available up to the time point t .

The intensities of the counting processes $N_{n,ij}$ are modelled by

$$\lambda_{n,ij}(\theta, t) := G(\theta; (Y_{n,ij}(s))_{i,j=1,\dots,n} : s \leq t),$$

where $Y_{n,ij}(t)$ are \mathcal{F}_t -predictable co-variates. Andersen et al. (1993) shows the following form of the log-likelihood for the parameter θ :

$$\ell_T(\theta) = \sum_{0 < t \leq T} \sum_{(i,j) \in L_n} \Delta N_{n,ij}(t) \log \lambda_{n,ij}(\theta, t) - \int_0^T \sum_{(i,j) \in L_n} \lambda_{n,ij}(\theta, t) dt,$$

and hence, we obtain the maximum likelihood estimator as

$$\hat{\theta} := \arg \max_{\theta \in \Theta} \ell_T(\theta),$$

where Θ denotes the range in which the true parameter is located.

The above approach is quite flexible and general. In order to be more specific, and for modelling reasons explained shortly, we will, in the following, assume that G has the following Cox-type form

$$G(\theta; (C_{n,ij}(s), Y_{n,ij}(s))_{i,j=1,\dots,n} : s \leq t) = C_{n,ij}(t) \exp(\theta^T Y_{n,ij}(t)), \quad (2.1)$$

where the functions $C_{n,ij}(t)$ are indicator functions only taking values in $\{0, 1\}$, and they are assumed to be predictable.

This particular type of intensity allows for a nice interpretation of the parameters: The intensity has the form $\prod_{k=1}^q e^{\theta_k Y_{n,ij}^{(k)}(t)}$, where $Y_{n,ij}^{(k)}(t)$ denotes the k -th component of $Y_{n,ij}(t)$. Hence, θ_k quantifies the impact of $Y_{n,ij}^{(k)}(t)$ on the intensity, given that the remaining covariate vector stays the same. $C_{n,ij}(t)$ determines whether the pair (i, j) is at risk for an interaction at time t . We will assume that, with positive probability, links can form at any time $0 < t < T$, i.e., $\mathbb{P}(C_{n,ij}(t) = 1) > 0$. However, these probabilities may converge to zero as the network size n increases, e.g, in order to produce sparsity. The presence of the function $C_{n,ij}(t)$ enhances the modelling flexibility significantly. For instance, we can model them as being equal to zero for a certain subset of edges (i, j) not possessing a certain property at time t . One example is, to set $C_{n,ij}(t)$ equal to zero, if there was no event between i and j for a certain period $\Delta t = (t - \delta, t)$ for some $\delta > 0$. In this case our model is only fitted to "active" pairs, and for pairs with low activity one may look for a

different model. Thus a proper choice of $C_{n,ij}(t)$ allows to split up the analysis into different regimes. The use of these modelling ideas is illustrated in our empirical study, presented in section 3.

Cox-type intensities are also considered in Perry and Wolfe (2013), in a similar model. However, there the estimation is based on a partial likelihood, which models the occurrence of directed events originating from a node j , assuming that such events exist. Their model, and consequently also their resulting estimators, are different from ours. Moreover, Perry and Wolfe (2013) do not consider the case of the parameters depending on time t , which we will do in the next subsection. Another related model can be found in Leenders (1995) and Butts (2008), but the focus of their work is more on the empirical application of the model to a social sciences problems, rather than their rigorous analysis.

2.2 Estimation in time-varying coefficient models

In time series applications, it turns out that powerful fits can be achieved by letting the time series parameters depend on time, and this is what we consider here as well. We will use the above model with θ in (2.1) depending on t , or in other words, $\theta = \theta(t)$ is now a parameter function.

An estimator of this parameter function at a given point t_0 can be obtained by maximizing the following local likelihood function

$$\begin{aligned} \ell_T(\mu, t_0) = & \sum_{0 < t \leq T} \frac{1}{h} K\left(\frac{t-t_0}{h}\right) \sum_{(i,j) \in L_n} \Delta N_{n,ij}(t) \log \lambda_{n,ij}(\mu, t) \\ & - \int_0^T \sum_{(i,j) \in L_n} \frac{1}{h} K\left(\frac{t-t_0}{h}\right) \lambda_{n,ij}(\mu, t) dt, \end{aligned} \quad (2.2)$$

where K is a kernel function (positive and integrating to one), and $h = h_n$ is the bandwidth. The corresponding local MLE is defined as

$$\hat{\theta}(t_0) = \arg \max_{\theta \in \Theta} \ell_T(\theta, t_0), \quad (2.3)$$

with Θ modeling the range of the parameter functions. Recall that we use the following Cox-type form of the intensity:

$$\lambda_{n,ij}(\theta, t) = C_{n,ij}(t) \exp \{ \theta(t)^T Y_{n,ij}(t) \}. \quad (2.4)$$

Using the hazard functions from (2.4), the local log-likelihood can be written as:

$$\ell_T(\theta, t_0) = \sum_{i,j=1}^n \frac{1}{h} \left(\int_0^T K\left(\frac{t-t_0}{h}\right) \theta^T Y_{n,ij}(t) dN_{n,ij}(t) \right)$$

$$- \int_0^T K \left(\frac{t - t_0}{h} \right) C_{n,ij}(t) \exp(\theta^T Y_{n,ij}(t)) dt. \quad (2.5)$$

The maximum likelihood estimator $\hat{\theta}_n(t_0)$ studied in this paper, is defined as the maximizer of (2.5) over θ . Denote by $L_n(t_0)$ the set of active edges, i.e., the set of all pairs (i, j) , such that, $C_{n,ij}(t_0) = 1$. We denote by $|L_n(t_0)|$ the size of the set $L_n(t_0)$. Our main theoretical result, given below, says that for a given $t_0 \in (0, T)$, the maximum likelihood estimator $\hat{\theta}_n(t_0)$ exists, is asymptotically consistent, and is asymptotically normal.

To formulate our main result, the following technical assumptions are needed.

2.3 Assumptions

Our assumptions do not specify the dynamics of the covariables $Y_{n,ij}(t)$ and of the censoring variable $C_{n,ij}(t)$. Instead of this, we assume that the stochastic behaviour of these variables stabilizes for $n \rightarrow \infty$. More precisely, we make the following assumptions.

- (A1)** For every n and for any $t \in [t_0 - h, t_0 + h]$, the joint distribution of $(C_{n,ij}(t), Y_{n,ij}(t))$ is identical for all pairs (i, j) . Furthermore, for any $s, t \in [t_0 - h, t_0 + h]$, the conditional distribution of the covariate $Y_{n,ij}(t)$ given that $C_{n,ij}(s) = 1$, has a density $f_{s,t}(y)$ with respect to a measure μ on \mathbb{R}^q , and this conditional distribution does not depend on (i, j) and n . We use the shorthand notation f_s for $f_{s,s}$. Finally, it holds that: $n \rightarrow \infty$, $h \rightarrow 0$, $l_n := \frac{n(n-1)}{2} \mathbb{P}(C_{n,12}(t_0) = 1) \rightarrow \infty$, $l_n h \rightarrow \infty$, and $l_n h^5 = O(1)$.

Note that, $l_n = \frac{n(n-1)}{2} \cdot \mathbb{P}(C_{n,12}(t_0) = 1)$ is the effective sample size at time t_0 , because $\frac{n(n-1)}{2}$ is the number of possible links between vertices, of which, in average, we observe the fraction $\mathbb{P}(C_{n,12}(t_0) = 1)$. (For directed networks, one simply has to replace $\frac{n(n-1)}{2}$ by $n(n-1)$ in the definition of l_n .) With this in mind, the assumptions on the bandwidth are standard. The most restrictive assumption in (A1) is that the conditional distribution of $Y_{n,ij}(t)$, given $C_{n,ij}(s) = 1$, does not depend on i, j . Observe that this holds if the array of $(C_{n,ij}, Y_{n,ij})_{i,j}$ is jointly exchangeable in (i, j) for any fixed n . The additional assumption that the conditional distribution of $Y_{n,ij}(t)$, given $C_{n,ij}(s)$, does not change with n is not very restrictive, because it is natural to assume that the distribution depends only on the local structure of the network. For instance, if we assume that a fixed vertex i has only a bounded number of interaction partners j while the network grows, then it is natural to assume that the local structure given by the interacting partners does not undergo major changes for $n \rightarrow \infty$. We make this additional assumption mainly to avoid stating lengthy technical assumptions allowing to interchange the order of differentiation and integration at several places in the proof.

We add some standard assumptions on the kernel.

- (A2)** The kernel K is positive and supported on $[-1, 1]$, and it satisfies $\int_{-1}^1 K(u) du = 1$, $\int_{-1}^1 K(u) u du = 0$ and $\max_{-1 \leq u \leq 1} K(u) < \infty$.

The next condition makes smoothness assumptions for the parameter curve θ_0 and the density $f_s(y)$.

(A3) The parameter space Θ is compact and convex. Let $\tau := \sup_{\theta \in \Theta} \|\theta\| < \infty$. The parameter function $\theta_0(t)$ takes values in Θ , and, in a neighbourhood of t_0 , it is twice continuously differentiable. The value $\theta_0(t_0)$ lies in the interior of Θ .

We continue with some tail conditions on $f_s(y)$ and its derivatives. They are fulfilled if, e.g., the covariates are bounded.

(A4) For μ -almost all y , the density $f_s(y)$ is twice continuously differentiable in s . For an open neighbourhood U of t_0 and $U_h := [t_0 - h, t_0 + h]$ it holds for all pairs (i, j) and (k, l)

$$\int \sup_{s \in U} \left\{ (1 + \|y\| + \|y\|^2 + \|y\|^3) |f_s(y)| + (1 + \|y\| + \|y\|^2) \left| \frac{d}{ds} f_s(y) \right| \right. \quad (2.6)$$

$$\left. + (1 + \|y\|) \left| \frac{d^2}{ds^2} f_s(y) \right| + \|y\|^2 \cdot f_{s,t_0}(y) \right\} \cdot \exp(\tau \cdot \|y\|) d\mu(y) < \infty,$$

$$\sup_{s, t \in U_h} \mathbb{E} \left(\|Y_{n,ij}(s)\|^2 \cdot \|Y_{n,kl}(t)\|^2 \right. \quad (2.7)$$

$$\left. \cdot e^{\tau(\|Y_{n,ij}(s)\| + \|Y_{n,kl}(t)\|)} \Big| C_{n,ij}(t_0) = 1, C_{n,kl}(t_0) = 1 \right) = O(1),$$

$$\sup_{s \in U_h} \mathbb{E} \left(\|Y_{n,12}(s)\|^2 e^{\tau \|Y_{n,12}(s)\|} \Big| C_{n,12}(s) = 1, C_{n,12}(t_0) = 0 \right) = O(1), \quad (2.8)$$

$$\mathbb{E} \left(\sup_{s \in U_h} [\|Y_{n,12}(s)\| + \|Y_{n,12}(s)\|^2 + \|Y_{n,12}(s)\|^3 + \|Y_{n,12}(s)\|^4] \right. \quad (2.9)$$

$$\left. \cdot e^{\tau \|Y_{n,12}(s)\|} \Big| C_{n,12}(s) = 1 \right) < +\infty.$$

The next assumption guarantees identifiability.

(A5) $\theta^T Y_{n,12}(t_0) = 0$ a.s. (w.r.t. f_{t_0}) implies that $\theta = 0$.

The following assumption addresses the asymptotic behaviour of the distributions of the processes $C_{n,ij}(t)$. In particular, for t in a neighbourhood of t_0 , the assumptions address asymptotic stability of the marginal distributions of these processes, and on some kind of asymptotic independence of $C_{n,ij}$ and $C_{n,kl}$ for $|\{i, j\} \cap \{k, l\}| = 0$.

(A6) For $w(u) = K(u)$ and $w(u) = K^2(u) / \int K^2(v) dv$ it holds that

$$\int_{-1}^1 w(u) \frac{\mathbb{P}(C_{n,12}(t_0 + uh) = 1)}{\mathbb{P}(C_{n,12}(t_0) = 1)} du \rightarrow 1 \quad (2.10)$$

for $n \rightarrow \infty$. For

$$A_{n,ij,kl} := \int_{-1}^1 \int_{-1}^1 w(u)w(v) \frac{\mathbb{P}(C_{n,ij}(t_0 + uh) = 1, C_{n,kl}(t_0 + vh) = 1)}{\mathbb{P}(C_{n,12}(t_0) = 1)^2} dudv,$$

we assume that

$$A_{n,ij,kl} = \begin{cases} o(n^2) & \text{for } |\{i, j\} \cap \{k, l\}| = 2, \\ o(n) & \text{for } |\{i, j\} \cap \{k, l\}| = 1, \\ 1 + o(1) & \text{for } |\{i, j\} \cap \{k, l\}| = 0. \end{cases} \quad (2.11)$$

Furthermore, it holds that

$$\sup_{s \in [t_0 - h, t_0 + h]} \frac{\mathbb{P}(C_{n,12}(t_0) = 0, C_{n,12}(s) = 1)}{\mathbb{P}(C_{n,12}(s) = 1)} = o(h), \quad (2.12)$$

and for edges with $|\{i, j\} \cap \{k, l\}| \leq 1$

$$\frac{\mathbb{P}(C_{n,ij}(t_0) = 1, C_{n,kl}(t_0) = 1)}{(\mathbb{P}(C_{n,12}(t_0) = 1))^2} = O(1). \quad (2.13)$$

The next assumption involves $\theta_{0,n}$, defined as the maximizer of

$$\theta \mapsto \int_0^T \frac{1}{h} K\left(\frac{s - t_0}{h}\right) g(\theta, s) ds, \quad (2.14)$$

where g is defined in (A7). We show later that $\theta_{0,n}$ is uniquely defined, and that $\theta_{0,n}$ is close to $\theta_0(t_0)$ (see Lemma 4.2 and Proposition 4.2, respectively).

(A7) Define

$$\begin{aligned} \tau_{n,ij}(\theta, s) &= Y_{n,ij}(s) Y_{n,ij}(s)^T \exp(\theta^T Y_{n,ij}(s)), \\ g(\theta, t) &= \mathbb{E} [\theta^T Y_{n,ij}(t) \exp(\theta_0(t)^T Y_{n,ij}(t)) \\ &\quad - \exp(\theta^T Y_{n,ij}(t)) | C_{n,ij}(t) = 1] \end{aligned} \quad (2.15)$$

$$= \int_{\mathbb{R}^q} (\theta^T y e^{\theta_0(t)^T y} - e^{\theta^T y}) f_t(y) d\mu(y), \quad (2.16)$$

$$f_{n,1}(\theta, s, t | (i, j), (k, l)) = \mathbb{E}(\tau_{n,ij}(\theta, s) \tau_{n,kl}(\theta, t) | C_{n,ij}(s) = 1, C_{n,kl}(t) = 1),$$

$$f_2(\theta, t) = \mathbb{E}(\tau_{n,ij}(\theta, t) | C_{n,ij}(t) = 1) = -\partial_{\theta^2} g(\theta, t),$$

$$r_{n,ij}(s) = C_{n,ij}(s) Y_{n,ij}(s) \left(e^{\theta_0(s)^T Y_{n,ij}(s)} - e^{\theta_{0,n}^T Y_{n,ij}(s)} \right) - \partial_{\theta} g(\theta_{0,n}, s).$$

Note that, by Assumption (A1), f_2 and g do not depend on (i, j) and n . We assume that $f_{n,1}$ depends on (i, j) and (k, l) only through $|\{i, j\} \cap \{k, l\}|$. Moreover, we assume that, for all sequences $\theta_n \rightarrow \theta_0(t_0)$ and $u, v \in [-1, 1]$, it holds that $f_{n,1}(\theta_n, t_0 + uh, t_0 +$

$vh, (i, j), (k, l)$ converges to a value that depends only on $|\{i, j\} \cap \{k, l\}|$. We denote this limit by $f_1(\theta_0(t_0), |\{i, j\} \cap \{k, l\}|)$, and assume that

$$f_1(\theta_0(t_0), 0) = f_2(\theta_0(t_0), t_0)^2. \quad (2.17)$$

For the function $r_{n,ij}(s)$ we assume, for $|\{i, j\} \cap \{k, l\}| = 0$, that

$$\begin{aligned} \int_{-1}^1 \int_{-1}^1 K(u)K(v)\mathbb{E}(r_{n,ij}(t_0 + uh)r_{n,kl}(t_0 + vh)|C_{n,ij}(t_0) = 1, C_{n,kl}(t_0) = 1)dudv \\ = o((l_n h)^{-1}). \end{aligned} \quad (2.18)$$

Assumption (A7) specifies in which sense the covariates are asymptotically uncorrelated. It should be noted that, in all cases, the assumptions in (A7) refer only to those covariates which are observed, i.e., to those with $C_{n,ij}(t) = 1$. In particular, this means that, unconditional, $\tau_{n,ij}$ and $\tau_{n,kl}$ do not need to be uncorrelated. We only require that all correlation is transported through the censoring: The presence or absence of (i, j) can influence the presence or absence of (k, l) , but once we know that both are observed, the correlation vanishes asymptotically. For the vectors $r_{n,ij}$, we assume that their correlations vanish with a specified rate. This is justified because ultimately, we are only interested in $r_{n,ij}(s)$ when s is close to t_0 , and hence when $\theta_0(s)$ is close to $\theta_{0,n}$ as we shall prove later (without using this assumption). In fact, we will show that $\theta_{0,n} = \theta_0(s) + O(h)$. Moreover, the assumptions imply that the conditional expectation of $r_{n,ij}(s)$, given $C_{n,ij}(s) = 1$, is always equal to zero. So $r_{n,ij}$ is a small quantity which is then centered, and a weak independence will give the desired rate.

2.4 The main asymptotic result

Theorem 2.1. *Suppose that Assumptions (A1)–(A7) hold for a point $t_0 \in (0, T)$. Then, with probability tending to one, the derivative of the local log-likelihood function $\ell_T(\theta, t_0)$ has a root $\hat{\theta}_n(t_0)$, satisfying*

$$\sqrt{l_n h} \left(\hat{\theta}_n(t_0) - \theta_0(t_0) + \frac{1}{2} h^2 \Sigma^{-1} v \right) \rightarrow N \left(0, \int_{-1}^1 K(u)^2 du \Sigma^{-1} \right) \quad (2.19)$$

with

$$\begin{aligned} v &:= \int_{-1}^1 K(u)u^2 du \cdot \partial_\theta \partial_{t^2} g(\theta_0(t_0), t_0), \\ \Sigma &:= -\partial_{\theta^2} g(\theta_0(t_0), t_0). \end{aligned}$$

If, in addition, $\frac{|L_n(t_0)|}{l_n} \xrightarrow{\mathbb{P}} 1$, then l_n can be replaced by $|L_n(t_0)|$.

2.5 Direct network modelling

We consider the following general model for the link-based dynamics of a random network, using a multivariate continuous-time counting process approach allowing for arbitrary dependence structure between the links. As before let $V = \{1, \dots, n\}$ be the set of vertices and L_n be the set of all edges. Note that here we are considering undirected networks. But directed networks can be handled similarly. For a given link (i, j) , we let

$$Z_{n,ij}(t) = \begin{cases} 1 & \text{if link from } i \text{ to } j \text{ is present at time } t \\ 0 & \text{else.} \end{cases}$$

Then

$$Z_n(t) = (Z_{n,ij}(t))_{(i,j) \in L}$$

describes the random network, or, equivalently, the (upper half of the) adjacency matrix at time t . To describe the dynamics of the links over time we introduce two processes, $N_{n,ij}^+(t)$ and $N_{n,ij}^-(t)$, counting how often a link (i, j) was added or deleted, respectively, until time t . Formally,

$$\begin{aligned} N_{n,ij}^+(t) &= \#\{s \leq t : Z_{n,ij}(s) - Z_{n,ij}(s-) = 1\}, \\ N_{n,ij}^-(t) &= \#\{s \leq t : Z_{n,ij}(s) - Z_{n,ij}(s-) = -1\}. \end{aligned}$$

With these definitions, we can write, for $(i, j) \in L_n$,

$$Z_{n,ij}(t) = Z_{n,ij}(0) + N_{n,ij}^+(t) - N_{n,ij}^-(t).$$

For $v \in \{+, -\}$ the intensities of the counting processes $N_{n,ij}^v(t)$ are here defined as

$$\lambda_{n,ij}^v(\theta, t) = G_{n,ij}^v(\theta^v; (Z_n(s), Y_{n,ij}^v(s)) : s < t) \quad (2.20)$$

with

$$G_{n,ij}^+(\theta^+; (Z_n(s), Y_{n,ij}^+(s)) : s < t) = \gamma_{n,ij}^+(\theta^+; (Z_n(s), Y_{n,ij}^+(s)) : s < t) (1 - Z_{n,ij}(t-)), \quad (2.21)$$

$$G_{n,ij}^-(\theta^-; (Z_n(s), Y_{n,ij}^-(s)) : s < t) = \gamma_{n,ij}^-(\theta^-; (Z_n(s), Y_{n,ij}^-(s)) : s < t) Z_{n,ij}(t-) \quad (2.22)$$

for some functions γ^+ and γ^- respectively, where θ^+ and θ^- are two different parameters, determining the addition and the deletion processes, respectively. The vectors $Y_{n,ij}^v(t)$ for $v \in \{+, -\}$ denote covariates that are assumed to be \mathcal{F}_t -predictable. Note that this definition of the intensities makes sure that, as it should be, a link can only be added if none was present immediately before, and similarly for the removal for a link.

These definitions of the intensities fit into the framework of Section 2.2 with intensity function (2.4), when choosing $\lambda_{n,ij}^v(\theta^v, t) = C_{n,ij}^v(t) \cdot \exp(\theta^v(t)^T Y_{n,ij}^v(t))$ with $C_{n,ij}^v(t)$ being predictable $\{0, 1\}$ -valued processes that fulfill $C_{n,ij}^+(t) = 0$ if $Z_{n,ij}(t-) = 1$ and $C_{n,ij}^-(t) = 0$ if $Z_{n,ij}(t-) = 0$. Again, as in Section 2.2, we allow that the parameter is a function of time. To sum it up: The processes $N_{n,ij}^+$ are modelled with intensity $\lambda_{n,ij}^+(\theta_0^+, t)$ and the processes $N_{n,ij}^-$ are modelled with intensity function $\lambda_{n,ij}^-(\theta_0^-, t)$. Our model allows the covariates $Y_{n,ij}^v$ and the true parameter functions θ_0^v to be different for $v = '+'$ and $v = '-'$. For estimating the parameters we consider observations of the same type only, i.e., we will compute two maximum likelihood estimators: the estimator of $\theta_0^+(t)$ based on the processes N_{ij}^+ , and the estimator for θ_0^- based on the processes N_{ij}^- . Both estimators can be treated as coming from an interaction based model and hence the theory from Section 2.2 can be applied.

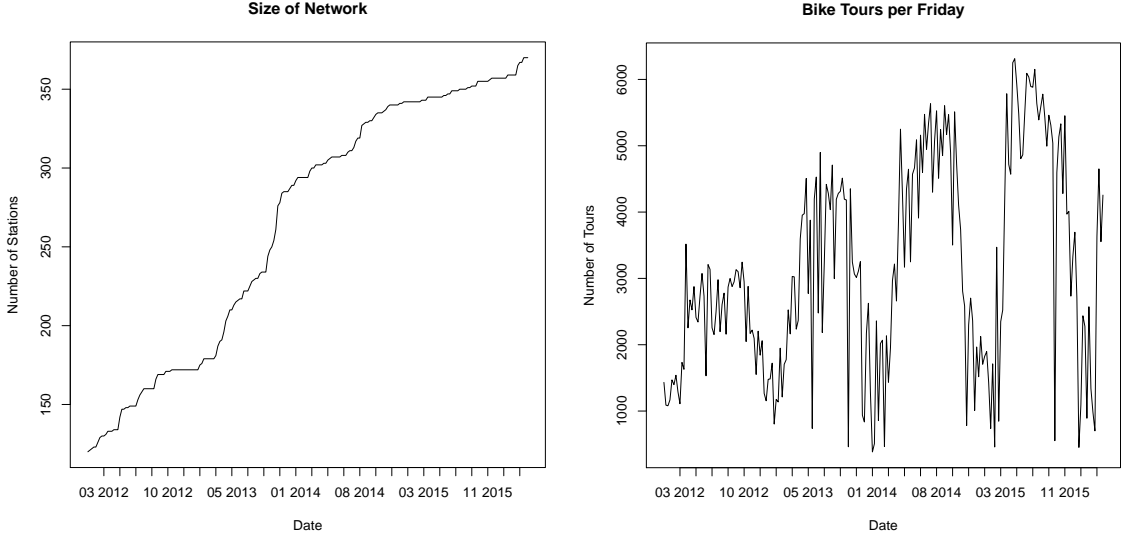
3 Application to Bike Data

To illustrate the finite sample performance of our estimation procedure described above, we are considering the Capital Bikeshare (CB) Performance Data, publicly available at <http://www.capitalbikeshare.com/system-data>. This data describes the usage of the CB-system at Washington D.C. from Jan. 2012 to March 2016. Using this data, we construct a network as follows. Each bike station j will become a node in our network, and edges between two stations i, j will be formed depending on whether a bike was rented at station i and returned to station j (or vice versa) at the same day. So, in our analysis, rentals over several days have been ignored, and also the direction of travel.

Figure 1 shows some summary statistics of the data. In Figure 1a, we see the number of available bike stations, which is strongly increasing. Figure 1b shows the number of bike tours on Fridays. An obvious periodicity is visible: The cycling activity is much lower in winter than during summer.

We aim at modelling the bike sharing activities on Fridays, seen on the right panel of Figure 1. We use the event counting approach from Section 2.1, where *event* here means that a bike is rented at station i and returned at station j , or vice versa. We will also refer to this event as a tour between i and j . In order to reduce computational complexity, we will introduce a discretisation of the process, thereby sacrificing the time continuity. However, effects like lower biking activity at night, can still be present in the data without effecting the estimation. We make this precise in the following.

Time t is measured in hours of consecutive Fridays. So, if k is the current week, and r is the time on Friday (in 24h), then $t := (k-1) \cdot 24 + r$. Thus, with $r_t := (t \bmod 24)$, the quantity $k_t := \frac{t-r_t}{24} + 1$ gives the week the time point t falls into. The processes $N_{i,j}(t)$, counting the number of tours between i and j on Fridays, are modelled as counting processes with intensities $\lambda_{i,j}(\theta(t), t) := \alpha(t) \exp(\theta^T Y_{i,j}(k_t)) \cdot C_{i,j}(k_t)$. The covariate vector $Y_{i,j}(k_t)$ and the censoring indicator $C_{i,j}(k_t)$ will be defined later. Note that they both only depend on



(a) Shows the number of available bike stations (b) Number of tours undertaken per Friday

Figure 1: Simple descriptive statistics of the bike data

k_t , i.e. on the current week, and not on the actual time on the Friday under consideration. The function α is 24 periodic and integrates to one over a period, i.e., $\alpha(t) = \alpha(t + 24)$ and $\int_t^{t+24} \alpha(s) ds = 1$. The function α is introduced to model the reasonable assumption that the activity varies during the day. Suppose now, that our target is the estimation of the parameter vector $\theta(t_0)$ with $t_0 = (k_{t_0} - 1)24 + r_0$ and $r_0 = 12$, say. We choose a piecewise constant kernel K with $K((24k+x)/h) = K(24k/h)$, for all $k \in \mathbb{N}$ and $0 \leq x < 24$. Plugging in these choices of the intensity and the kernel to the log-likelihood (2.2), we see that our maximum likelihood estimator maximizes the function

$$\theta \mapsto \sum_{k=0}^{k_T} K_\kappa(k - k_{t_0}) \theta^T Y_{i,j}(k) \int_{k \cdot 24}^{(k+1) \cdot 24} dN_{i,j}(t) + \sum_{k=0}^{k_T} K_\kappa(k - k_{t_0}) \exp(\theta^T Y_{i,j}(k)) C_{i,j}(k),$$

where $\int_{k \cdot 24}^{(k+1) \cdot 24} dN_{i,j}(t)$ gives the number of tours between i and j on the Friday in week k , and where $K_\kappa(k) = K(k/\kappa)$ with $\kappa = h/24$. In our empirical analysis, we chose $K_\kappa(k)$ as triangle weights with support $\{-\kappa, \dots, \kappa\}$ and considered only integer choices of the bandwidth κ . The bandwidth choice is discussed at the end of this section.

We explain now the choice of our covariate vector $Y_{i,j}$. Denote by $\Delta_{i,j}(k, d)$ the number of tours between i and j on day d in week k , where $d = 4$ means Monday and $d = 7$ refers to Thursday (for us the week starts on Fridays, i.e. Friday is $d = 1$). For $r \in (0, 1)$, we encode the activity between i and j in week k as $A_{i,j,k} = (1 - r) \sum_{d=4}^7 r^{7-d} \Delta_{i,j}(k, d)$ (mind the limits of the summation - Fridays are not included). In our simulations, we chose $r = 0.8$. We construct a network $G(k)$, for every week k , by connecting i and j , if and only

if, there was at least one tour on the Friday in that week. We denote by $I_{i,j,k}$ the number of common neighbours of i and j in the graph $G(k)$. We let $d_{i,k}$ be the degree of node i in $G(k)$, $T_{i,j,k}$ the number of tours between i and j on the Friday in the k -th week, and $T_{i,j,k,k-1} = (T_{i,j,k} + T_{i,j,k-1})/2$ the average number of tours on the two Fridays in weeks k and $k-1$. Finally we collect everything in the covariate vector:

$$Y_{i,j}(k) := (1, A_{i,j,k-1}, I_{i,j,k-1}, \max(d_{i,k-1}, d_{j,k-1}), T_{i,j,k-1,k-2}, \mathbb{1}(T_{i,j,k-1,k-2} = 0))^T.$$

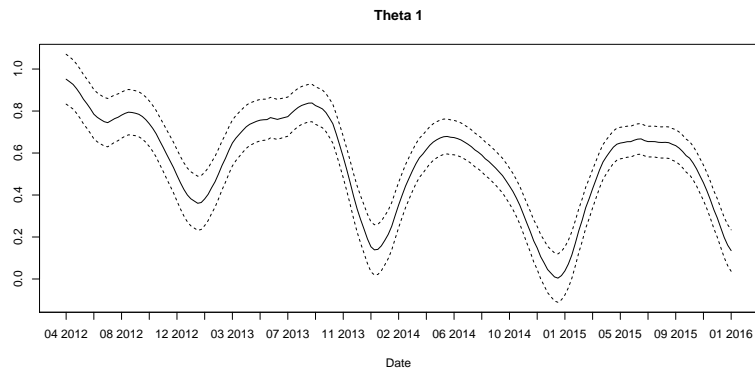
The censoring indicator function $C_{i,j}$ is defined to be equal to zero, if there was no tour between stations i and j in the last four weeks. In summary, we estimate a total of six parameter curves, corresponding to the effects of six covariates in our model:

- $\theta_1(t) \triangleq$ baseline
- $\theta_2(t) \triangleq$ activity between stations on previous week-days
- $\theta_3(t) \triangleq$ common neighbours of stations
- $\theta_4(t) \triangleq$ popularity of station, measured by degrees
- $\theta_5(t) \triangleq$ activity between stations on two previous Fridays
- $\theta_6(t) \triangleq$ inactivity between stations on two previous Fridays

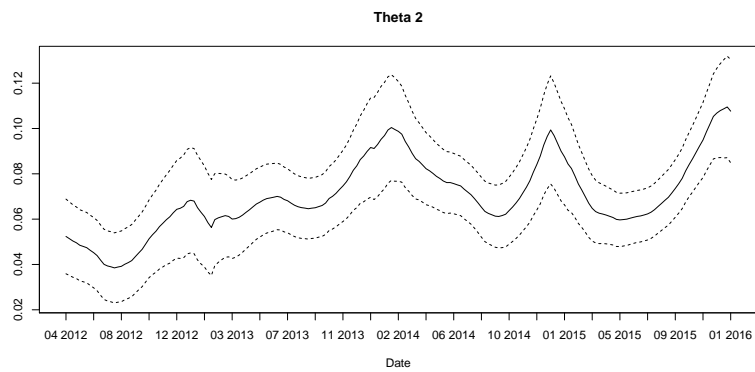
The resulting estimated parameter curves are shown in Figures 2 and 3. All calculations have been executed on the BwForCluster (cf. Acknowledgement). In all six parameter curves in Figures 2 and 3, we observe a clearly visible seasonality. Looking at Figure 2b, we see that importance of the activity in the week (Monday to Thursday) is higher during the winter months than in the summer. A plausible interpretation for this might be that the opportunist cyclists might be less active in winter because of the colder weather. So only those keep using a bike, who ride the same tour every day regardless of the weather. This makes the activity in the week a better predictor. Moreover, the weather in winter is more persistent, e.g., when there is snow it is likely to remain for a while.

Figure 2c shows that the number of common neighbours always has a significant positive effect on the hazard. This reflects the empirical finding that observed networks cluster more than totally random networks (e.g. see Jackson, 2008).

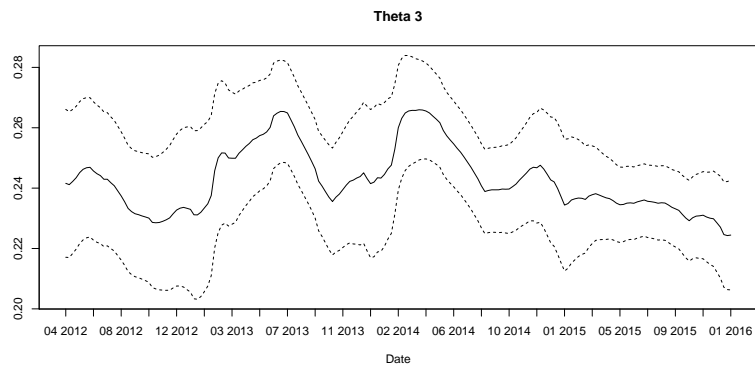
The influence of the popularity of the involved bike stations is investigated in Figure 3a (measured by the degree of the bike station). Interestingly, it always has a significant negative impact. The size of the impact is higher in the summer months, which again supports the hypothesis that in summer the behaviour of the network as a whole appears *more random* than in winter. But still, the negative impact is a bit unforeseen. This finding can be interpreted as the observed network having no hubs. Another reason for this effect might be, that stations can only host a fixed number of bikes: If a station i is empty, no new neighbours can be formed. A similar saturation effect happens if a lot of bikes arrive at station i . Moreover, it is plausible that effects caused by the degrees are already included in



(a) Estimate and confidence bands for $\theta_1(t)$

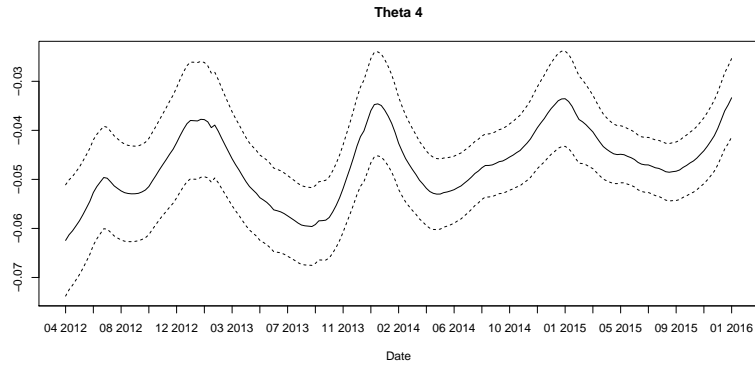


(b) Estimate and confidence bands for $\theta_2(t)$

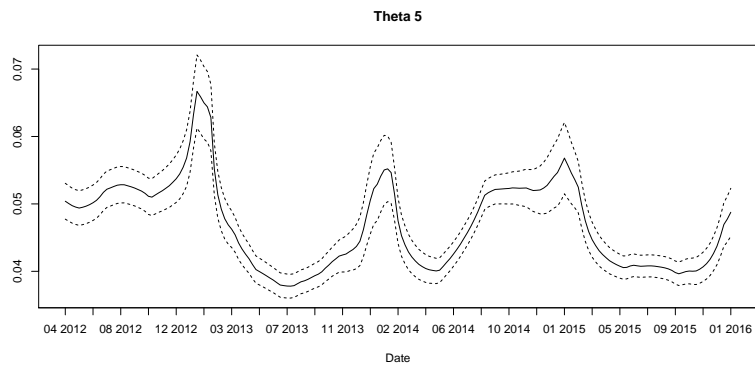


(c) Estimate and confidence bands for $\theta_3(t)$

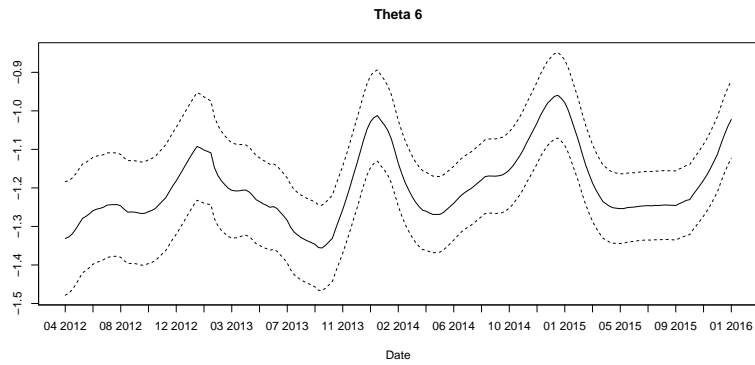
Figure 2: Estimates of $\theta_1(t)$, $\theta_2(t)$ and $\theta_3(t)$. The dotted lines indicate (pointwise) 99% confidence regions (plus minus 2.58 times the asymptotic standard deviation).



(a) Estimate and confidence bands for $\theta_4(t)$



(b) Estimate and confidence bands for $\theta_5(t)$



(c) Estimate and confidence bands for $\theta_6(t)$

Figure 3: Estimates of $\theta_4(t)$, $\theta_5(t)$ and $\theta_6(t)$. The dotted lines indicate (pointwise) 99% confidence regions (plus minus 2.58 times the asymptotic standard deviation).

2b, as well as in Figure 3b. They show the effect of the bike rides on the days immediately preceding the current Friday, and the effect of the average number of bike tours on the last two Fridays, respectively. In Figure 3b, we observe a similar behaviour as in Figure 2b (even more pronounced): In summer the predictive power of the tours on the last two Fridays is significantly lower than in winter, underpinning the theory that the destinations in summer tend to be based on more spontaneous decisions. Finally, in Figure 3c, we observe that no bike tours on the last two Fridays between a given pair of stations always has a significant negative impact on the hazard. Again a very plausible finding.

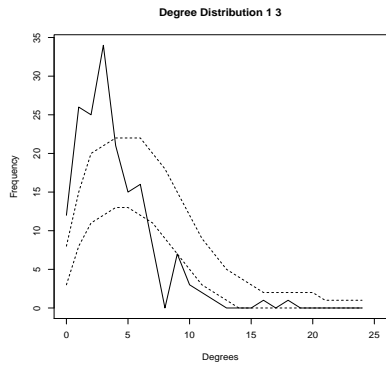
MODELLING OTHER NETWORK CHARACTERISTICS. In stochastic network analysis, a central strand of research is concerned with the question of whether characteristics observed in real networks can be adequately mimicked by stochastic network models. Important characteristics are degree distribution, clustering coefficient and diameter, and it is well-known, that it is challenging for network models (e.g., preferential attachment, small world models, configuration model) to adequately mimic the distributions of all these three characteristics simultaneously (see e.g. Jackson, 2008, or Zafarni et al., 2014). In order to see in how much our fitted model is able to capture these characteristics, we have simulated 3840¹ networks corresponding to three randomly chosen days, by using the network model with the fitted parameters of the corresponding day. We then compared the simulated three characteristics on these three days to the ones observed in the networks. Here, we present the results for the degree distribution on 7th December 2012. The other results are reported in the supplementary section.

In our analysis, we consider fitting sub-networks defined by the popularity of their edges: For given values $0 \leq l_1 < l_2 \leq \infty$, the network is constructed by placing an edge between a pair of nodes (i, j) , if the number of tours between i and j falls between l_1 and l_2 . Different ranges of l_1 and l_2 are considered. The idea is to consider the network of low frequented tours (for $l_1 = 1$ and $l_2 = 3$) up to the network of highly frequented tours (for $l_1 = 10$ and $l_2 = \infty$).

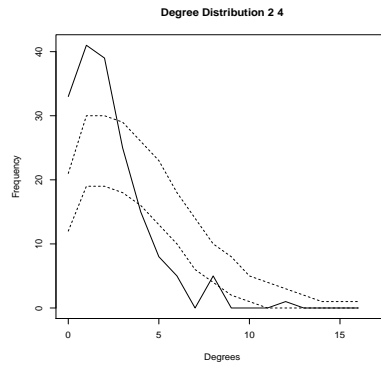
Figure 4 shows the simulated degree distributions for six different choices of l_1 and l_2 . The dotted lines indicate 10% and 90% quantiles of the simulated graphs, and the solid line shows the true degree distribution. We see that, in all six cases, the approximation is reasonable accurate, in particular if one takes into account that we did not specifically aim at reproducing the degree distributions. The plots show that the largest degree of the simulated networks and the observed network lie not too far from each other, and the overall shape of the degree distribution is captured well. It should also be noted that we used only six covariates, whereas in other related empirical work much higher dimensional models have been used, see e.g. the discussions in Perry and Wolfe (2013).

BRIEF REMARK ON CHOICE OF BANDWIDTH VIA ONE-SIDE CROSS VALIDATION. To choose the bandwidth, we calculate a local linear estimate with a one-sided kernel $K_{+, \kappa}(k) =$

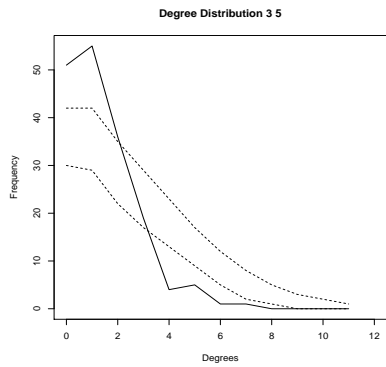
¹We chose to simulate 3840 networks, because we had 32 cores available, and on each of the cores we ran 120 predictions, which could be done in reasonable time.



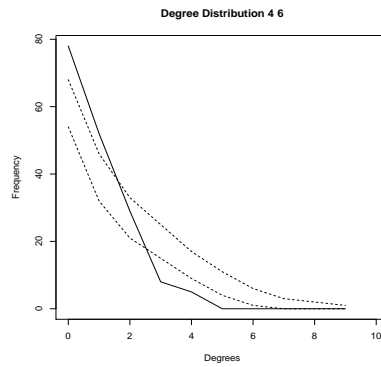
(a) Only edges with tour frequency between one and three



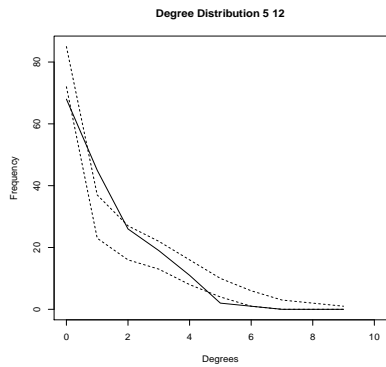
(b) Only edges with tour frequency between two and four



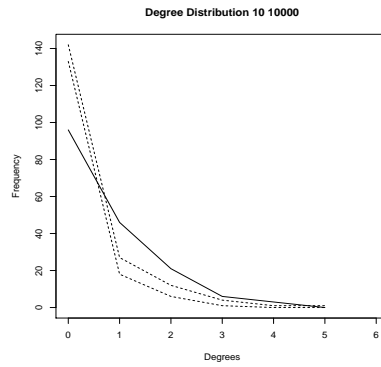
(c) Only edges with tour frequency between three and five



(d) Only edges with tour frequency between four and six



(e) Only edges with tour frequency between five and twelve



(f) Only edges with tour frequency larger than ten

Figure 4: Simulated degree distributions of sub-networks with different tour frequencies (see individual caption) for 7th December 2012. Dotted lines show 10% and 90% quantiles of simulations and solid line shows true distributions.

$K_\kappa(k)\mathbb{1}(k < 0)$. For all values of κ , the fitted value of the conditional expectation of $Y_{i,j}(k_{t_0})$, given the past, is compared with the outcome of $Y_{i,j}(k_{t_0})$. This is done for all non-censored edges. The results for different bandwidths are shown in Figure 5. We see that the prediction error of the model decreases, until we reach the bandwidth $\kappa = 23$. In one-sided cross-validation, one now makes use of the fact that the ratio of asymptotically optimal bandwidths of two kernel estimators with different kernels, K and L is equal to $\rho = [\int K^2(u)du(\int u^2L(u)du)^2(\int L^2(u)du)^{-1}(\int u^2K(u)du)^{-2}]^{1/5}$. For a triangular kernel, and its one-sided version, we get $\rho \approx 1.82$. The one-sided CV bandwidth is given by dividing 23 by ρ which yields bandwidth roughly twelve (here we also only consider integer bandwidths). More details on the one-sided cross-validation approach are presented in the supplementary material.

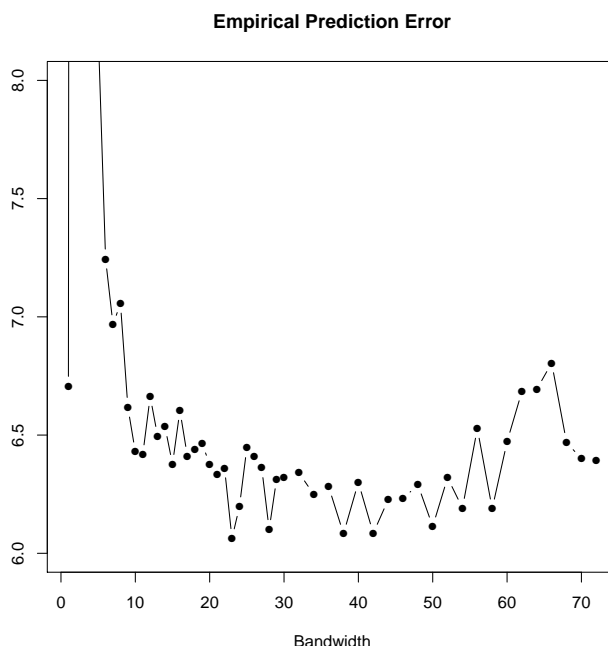


Figure 5: Mean Squared Prediction Error for different bandwidths.

4 Proof of Theorem 2.1

In the proof, we do not distinguish explicitly directed and undirected networks: in the undirected case, we always assume $i < j$, moreover we will need $l_n = O(n^2\mathbb{P}(C_{n,12}(t_0) = 1))$, which is true in both cases. The processes $N_{n,ij}$ are counting processes with intensity given by $\lambda_{n,ij}(\theta_0(t), t)$. We can decompose these counting processes as (Doob-Meyer Decomposi-

tion, see e.g. Andersen et al.(1993) Chapter II.4)

$$N_{n,ij}(t) = M_{n,ij}(t) + \int_0^t \lambda_{n,ij}(\theta_0(s), s) ds, \quad (4.1)$$

where $M_{n,ij}$ is a local, square integrable martingale. We use this decomposition of the counting processes in order to decompose the likelihood and its derivatives. Let $P_n(\theta)$ be defined as

$$P_n(\theta) := \frac{1}{l_n h} \sum_{i,j=1}^n \int_0^T K\left(\frac{s-t_0}{h}\right) C_{n,ij}(s) [\theta^T Y_{n,ij}(s) \exp(\theta_0(s)^T Y_{n,ij}(s)) - \exp(\theta^T Y_{n,ij}(s))] ds. \quad (4.2)$$

Note that we do not make the dependence of $P_n(\theta)$ on t_0 explicit in the notation. Using $P_n(\theta)$, we can write

$$\frac{1}{l_n} \ell(\theta, t_0) = \frac{1}{l_n h} \sum_{i,j=1}^n \int_0^T K\left(\frac{t-t_0}{h}\right) \theta^T Y_{n,ij}(t) dM_{n,ij}(t) + P_n(\theta), \quad (4.3)$$

$$\frac{1}{l_n} \cdot \frac{\partial}{\partial \theta} \ell(\theta, t_0) = \frac{1}{l_n h} \sum_{i,j=1}^n \int_0^T K\left(\frac{t-t_0}{h}\right) Y_{n,ij}(t) dM_{n,ij}(t) + P'_n(\theta), \quad (4.4)$$

$$\frac{1}{l_n} \cdot \frac{\partial^2}{\partial \theta^2} \ell(\theta, t_0) = P''_n(\theta). \quad (4.5)$$

Recall that $\theta_{0,n}$ is defined as the maximizer of $\theta \mapsto \int_0^T \frac{1}{h} K\left(\frac{s-t_0}{h}\right) g(\theta, s) ds$, where g is defined in (A7). Note that the function g does not depend on n , see Assumption (A1). Lemma 4.2 shows that $\theta_{0,n}$ is uniquely defined. The value $\theta_{0,n}$ is the deterministic counterpart of the random quantity $\tilde{\theta}_n(t_0)$ that is defined as the solution of $P'_n(\tilde{\theta}_n(t_0)) = 0$. The existence of the latter is considered in Proposition 4.3.

Lemma 4.1. *We have*

$$\begin{aligned} & \theta^T y \exp(\theta_0(s)^T y) - \exp(\theta^T y) \\ & \leq \theta_0(s)^T y \exp(\theta_0(s)^T y) - \exp(\theta_0(s)^T y). \end{aligned}$$

Equality holds, if and only if, $\theta_0(s)^T y = \theta^T y$. In particular, $\theta_0(s)$ is the unique maximiser of $\theta \mapsto g(\theta, s)$.

Proof. Note that, for arbitrary $y \in \mathbb{R}$,

$$\frac{d}{dx} (xe^y - e^x) = e^y - e^x$$

implies that the differentiable function $x \mapsto xe^y - e^x$ has the unique maximizer $x = y$. This also implies the second statement of the lemma. \square

In all lemmas and propositions of this section, we assume that Assumptions (A1)–(A7) hold.

Fact 4.1. *For $j \in \{0, 1, 2\}, k \in \{0, 1, 2, 3\}$, with $j + k \leq 3$, the partial derivatives of order j of the function $g(\theta, s)$ with respect to s , and of order k with respect to θ , exist, for t in a neighbourhood of t_0 , and $\theta \in \Theta$. The partial derivatives can be calculated by interchanging the order of integration and differentiation in (2.16). For $\theta \in \Theta$ and s in a neighborhood of t_0 , all these partial derivatives of $g(\theta, s)$ are absolutely bounded. For the calculation of the first two derivatives of g with respect to θ , differentiation and application of the expectation operator can be interchanged in (2.15). The matrix Σ is invertible.*

Proof. The statement of this fact follows immediately from (2.6) of Condition (A4). Note that the functions θ_0, θ'_0 and θ''_0 are absolutely bounded in a neighbourhood of t_0 . This holds because these functions are continuous in a neighbourhood of t_0 , see (A3). \square

Lemma 4.2. *For n large enough, $\theta_{0,n}$ is uniquely defined, and it holds that $\theta_{0,n} \rightarrow \theta_0(t_0)$ as $n \rightarrow \infty$.*

Proof of Lemma 4.2. From Fact 4.1, we know that $\partial_t g(\theta, t)$ is absolutely bounded for t in a neighbourhood of t_0 and $\theta \in \Theta$. This implies that $\theta \mapsto \int_0^T \frac{1}{h} K\left(\frac{s-t_0}{h}\right) g(\theta, s) ds$ converges to $g(\theta, t_0)$, uniformly for $\theta \in \Theta$. Because $\partial_{\theta^2} g(\theta, t)$ is negative definite, this implies the statement of the lemma. \square

Lemma 4.3. *With $\Sigma_n = -\int_{-1}^1 K(u) \int_0^1 \partial_{\theta^2} g(\theta_0(t_0) + \alpha(\theta_{0,n} - \theta_0(t_0)), t_0 + uh) d\alpha du$, we have*

$$\Sigma_n \rightarrow \Sigma \text{ as } n \rightarrow \infty.$$

Moreover, the sequence

$$v_n = 2 \int_{-1}^1 K(u) \int_0^1 (1 - \alpha) \frac{d^2}{dt^2} \partial_{\theta} g(\theta_0(t_0), t_0 + (1 - \alpha)uh) u^2 d\alpha du$$

is bounded, and it holds that $v_n \rightarrow v$, as $n \rightarrow \infty$.

Proof. Using Lemmas 4.2 and Fact 4.1, we conclude that the integrand

$$\partial_{\theta^2} g(\theta_0(t_0) + \alpha(\theta_{0,n} - \theta_0(t_0)), t_0 + uh) \rightarrow \partial_{\theta^2} g(\theta_0(t_0), t_0)$$

(note that $u \in [-1, 1]$ and $\alpha \in [0, 1]$). The first statement of the lemma follows by an application of Lebesgue's Dominated Convergence Theorem, and the fact that $\partial_{\theta^2} g$ is bounded as a continuous function on a compact set. The second statement of the lemma follows similarly. \square

Proposition 4.2. *We have, for $t_0 \in (0, T)$,*

$$\theta_{0,n} = \theta_0(t_0) + h^2 \Sigma^{-1} v + o(h^2).$$

Proof of Proposition 4.2. Since $\theta_0(s)$ maximizes $\theta \mapsto g(\theta, s)$ (cf. Lemma 4.1), we have $\partial_\theta g(\theta_0(s), s) = 0$. Furthermore, by definition of $\theta_{0,n}$, we have $\int_0^T K\left(\frac{s-t_0}{h}\right) \partial_\theta g(\theta_{0,n}, s) ds = 0$. Having observed that, we compute, for h small enough,

$$\begin{aligned}
0 &= \frac{1}{h} \int_0^T K\left(\frac{s-t_0}{h}\right) \partial_\theta g(\theta_{0,n}, s) ds \\
&= \int_{-1}^1 K(u) \partial_\theta g(\theta_{0,n}, t_0 + uh) du \\
&= \int_{-1}^1 K(u) \left[\partial_\theta g(\theta_0(t_0), t_0 + uh) \right. \\
&\quad \left. + \int_0^1 \partial_{\theta^2} g(\theta_0(t_0) + \alpha(\theta_{0,n} - \theta_0(t_0)), t_0 + uh) d\alpha(\theta_{0,n} - \theta_0(t_0)) \right] du \\
&= \int_{-1}^1 K(u) \partial_\theta g(\theta_0(t_0), t_0 + uh) du + \Sigma_n(\theta_{0,n} - \theta_0(t_0)). \tag{4.6}
\end{aligned}$$

Σ_n converges to the invertible matrix Σ by Lemma 4.3. The first integral is of order h^2 . This follows by a Taylor expansion in the time parameter:

$$\begin{aligned}
&\int_{-1}^1 K(u) \partial_\theta g(\theta_0(t_0), t_0 + uh) du \\
&= \int_{-1}^1 K(u) \left[\partial_\theta g(\theta_0(t_0), t_0) + \frac{d}{dt} g_\theta(\theta_0(t_0), t_0) uh + \right. \\
&\quad \left. \int_0^1 (1-\alpha) \frac{d^2}{dt^2} \partial_\theta g(\theta_0(t_0), t_0 + (1-\alpha)uh) d\alpha u^2 h^2 \right] du \\
&= \frac{1}{2} h^2 v_n.
\end{aligned}$$

By Lemma 4.3, v_n is bounded. Thus, together with (4.6), we have established

$$\theta_{0,n} = \theta_0(t_0) - (\Sigma_n^{-1} - \Sigma^{-1} + \Sigma^{-1}) \frac{1}{2} h^2 v_n = \theta_0(t_0) - \frac{1}{2} h^2 \Sigma^{-1} v_n - \frac{1}{2} h^2 (\Sigma_n^{-1} - \Sigma^{-1}) v_n.$$

The statement of the proposition now follows from $v_n \rightarrow v$. □

Lemma 4.4. *We have*

$$P'_n(\theta_{0,n}) \xrightarrow{\mathbb{P}} 0. \tag{4.7}$$

For any $k, l \in \{1, \dots, q\}$, it holds that

$$P''_n(\theta_{0,n}) \xrightarrow{\mathbb{P}} -\Sigma. \tag{4.8}$$

Moreover,

$$\sup_{k,l,r,\theta} \left| \frac{\partial^2}{\partial \theta_k \partial \theta_l} P_n^{(r)}(\theta) \right| = O_P(1), \tag{4.9}$$

where $P_n^{(r)}$ denotes the r -th component of P'_n , the supremum runs over $k, l, r \in \{1, \dots, q\}$, and $\theta \in \Theta$.

Proof. We start by showing that $P'_n(\theta_{0,n}) = o_P(1)$. This holds, if $\mathbb{E}(\|P'_n(\theta_{0,n})\|) = o(1)$. Define $\rho_{n,ij}(\theta, s) := \|Y_{n,ij}(s)\| \cdot |\exp(\theta_0(s)^T Y_{n,ij}(s)) - \exp(\theta^T Y_{n,ij}(s))|$. By positivity of $\rho_{n,ij}(\theta, s)$, we may apply Fubini's Theorem, and thus we compute

$$\begin{aligned} & \mathbb{E}(\|P'_n(\theta_{0,n})\|) \\ & \leq \frac{1}{l_n} \sum_{i,j=1}^n \int_{-1}^1 K(u) \mathbb{E}(C_{n,ij}(t_0 + uh) \rho_{n,ij}(\theta_{0,n}, t_0 + uh)) du \\ & = \frac{1}{l_n} \sum_{i,j=1}^n \int_{-1}^1 K(u) \mathbb{P}(C_{n,ij}(t_0 + uh) = 1) \mathbb{E}(\rho_{n,ij}(\theta_{0,n}, t_0 + uh) | C_{n,ij}(t_0 + uh) = 1) du. \end{aligned}$$

The expectation in the integral expression can be bounded by applying a Taylor expansion:

$$\begin{aligned} & \mathbb{E}(\rho_{n,ij}(\theta_{0,n}, s_u) | C_{n,ij}(s_u) = 1) \\ & \leq \mathbb{E} \left(\|Y_{n,ij}(s_u)\|^2 \int_0^1 \exp([\theta_0(s_u) - \alpha \cdot (\theta_0(s_u) - \theta_{0,n})]^T Y_{n,ij}(s_u)) d\alpha \Big| C_{n,ij}(s_u) = 1 \right) \\ & \quad \times \|\theta_0(s_u) - \theta_{0,n}\|, \end{aligned}$$

where $s_u = t_0 + uh$. Now, by (2.9) in Assumption (A4), the expectation in the last upper bound is bounded by a constant C , uniformly in $u \in [-1, 1]$. Using $\sup_{u \in [-1, 1]} \|\theta_0(t_0 + uh) - \theta_{n,0}\| = o(1)$, we obtain

$$\begin{aligned} & \mathbb{E}(\|P'_n(\theta_{0,n})\|) \\ & \leq \frac{1}{l_n} \sum_{i,j=1}^n \int_{-1}^1 K(u) \mathbb{P}(C_{n,ij}(t_0 + uh) = 1) du \cdot C \cdot \sup_{v \in [-1, 1]} \|\theta_0(t_0 + vh) - \theta_{0,n}\| \\ & = C \cdot \mathbb{P}(C_{n,ij}(t_0) = 1)^{-1} \cdot \int_0^1 K(u) \mathbb{P}(C_{n,ij}(t_0 + uh) = 1) du \cdot o(1) \\ & = o(1), \end{aligned}$$

where the last equality is a consequence of (2.10). This shows (4.7).

We now show (4.8). With $\partial_{\theta^2} g(\theta_{0,n}, s) = -\mathbb{E}(\tau_{n,ij}(\theta_{0,n}, s) | C_{n,ij}(s) = 1)$, Fact 4.1 gives

$$\mathbb{E}(P''_n(\theta_{0,n})) = -\frac{1}{l_n h} \sum_{i,j=1}^n \int_0^T K\left(\frac{s-t_0}{h}\right) \mathbb{P}(C_{n,ij}(s) = 1) \mathbb{E}(\tau_{n,ij}(\theta_{0,n}, s) | C_{n,ij}(s) = 1) ds.$$

For (4.8), it suffices to show:

$$P''_n(\theta_{0,n}) - \mathbb{E}(P''_n(\theta_{0,n})) = o_P(1), \quad (4.10)$$

$$\mathbb{E}(P''_n(\theta_{0,n})) + \Sigma = o(1). \quad (4.11)$$

For the proof of (4.11), we note that with $a_n(u) = \frac{\mathbb{P}(C_{n,12}(t_0+uh)=1)}{\mathbb{P}(C_{n,12}(t_0)=1)}$,

$$\mathbb{E}(P''_n(\theta_{0,n})) + \Sigma$$

$$\begin{aligned}
&= \int_{-1}^1 K(u) [a_n(u) \partial_{\theta^2} g(\theta_{0,n}, t_0 + uh) - \partial_{\theta^2} g(\theta_0(t_0), t_0)] du \\
&= \int_{-1}^1 K(u) a_n(u) [\partial_{\theta^2} g(\theta_{0,n}, t_0 + uh) - \partial_{\theta^2} g(\theta_0(t_0), t_0)] du \\
&\quad + \partial_{\theta^2} g(\theta_0(t_0), t_0) \int_{-1}^1 K(u) (a_n(u) - 1) du \\
&= o(1).
\end{aligned}$$

Here we use (2.10), and $\theta_{0,n} - \theta_0(t_0) = o(1)$ (see Proposition 4.2).

For the proof of (4.10), we write

$$\begin{aligned}
&P_n''(\theta_{0,n}) - \mathbb{E}(P_n''(\theta_{0,n})) \\
&= \frac{1}{l_n h} \sum_{i,j=1}^n \int_0^T K\left(\frac{s-t_0}{h}\right) [-C_{n,ij}(s) \tau_{n,ij}(\theta_{0,n}, s) + \mathbb{P}(C_{n,ij}(s) = 1) \partial_{\theta^2} g(\theta_{0,n}, s)] ds.
\end{aligned}$$

We will apply Markov's inequality to show that this term converges to zero. When squaring the above sum, we can split the resulting double sum into three parts, depending on whether $|\{i, j\} \cap \{k, l\}| = 0, 1$ or 2 . Thus we have to show that the following three sequences converge to zero:

$$\mathbb{E}\left(\frac{1}{l_n^2 h^2} \sum_{(i,j)} \bar{\kappa}_{n,ij}(\theta_{0,n})^2\right) = o(1), \tag{4.12}$$

$$\mathbb{E}\left(\frac{1}{l_n^2 h^2} \sum_{\substack{(i,j),(k,l) \\ \text{sharing one vertex}}} \bar{\kappa}_{n,ij}(\theta_{0,n}) \bar{\kappa}_{n,kl}(\theta_{0,n})\right) = o(1), \tag{4.13}$$

$$\mathbb{E}\left(\frac{1}{l_n^2 h^2} \sum_{\substack{(i,j),(k,l) \\ \text{sharing no vertex}}} \bar{\kappa}_{n,ij}(\theta_{0,n}) \bar{\kappa}_{n,kl}(\theta_{0,n})\right) = o(1), \tag{4.14}$$

where $\kappa_{n,ij}(\theta_{0,n}, s) := -C_{n,ij}(s) \tau_{n,ij}(\theta_{0,n}, s) + \mathbb{P}(C_{n,ij}(s) = 1) \partial_{\theta^2} g(\theta_{0,n}, s)$, and $\bar{\kappa}_{n,ij}(\theta_{0,n}) := \int_0^T K\left(\frac{s-t_0}{h}\right) \kappa_{n,ij}(\theta_{0,n}, s) ds$. Now note that

$$\begin{aligned}
&\mathbb{E}(\bar{\kappa}_{n,ij}(\theta_{0,n}) \bar{\kappa}_{n,kl}(\theta_{0,n})) \\
&= \int_{-1}^1 \int_{-1}^1 K(u) K(v) \mathbb{E}(\kappa_{n,ij}(\theta_{0,n}, t_0 + uh) \kappa_{n,kl}(\theta_{0,n}, t_0 + vh)) dudv,
\end{aligned}$$

and that the sum in (4.12) has $O(n^2)$ terms, (4.13) comprises $O(n^3)$ terms, and finally (4.14) has $O(n^4)$ terms (these orders are true for both: directed and undirected networks). Thus, it is sufficient to show that

$$\mathbb{P}(C_{n,12}(t_0) = 1)^{-2} \int_{-1}^1 \int_{-1}^1 K(u) K(v) \mathbb{E}(\kappa_{n,ij}(\theta_{0,n}, t_0 + uh) \kappa_{n,kl}(\theta_{0,n}, t_0 + vh)) dudv$$

$$= \begin{cases} o(n^2) & \text{for } |\{i, j\} \cap \{k, l\}| = 2 \\ o(n) & \text{for } |\{i, j\} \cap \{k, l\}| = 1 \\ o(1) & \text{for } |\{i, j\} \cap \{k, l\}| = 0. \end{cases} \quad (4.15)$$

For the proof of (4.15), we note that

$$\mathbb{E}(\kappa_{n,ij}(\theta_{0,n}, t_0 + uh)\kappa_{n,kl}(\theta_{0,n}, t_0 + vh)) = T_{n,1}(u, v) - T_{n,2}(u, v),$$

where

$$\begin{aligned} T_{n,1}(u, v) &= \mathbb{P}(C_{n,ij}(t_0 + uh) = 1, C_{n,kl}(t_0 + vh) = 1) \\ &\quad \times f_{n,1}(\theta_{0,n}, t_0 + uh, t_0 + vh | (i, j), (k, l)), \\ T_{n,2}(u, v) &= \mathbb{P}(C_{n,ij}(t_0 + uh) = 1)\mathbb{P}(C_{n,kl}(t_0 + vh) = 1) \\ &\quad \times f_2(\theta_{0,n}, t_0 + uh)f_2(\theta_{0,n}, t_0 + vh). \end{aligned}$$

We get

$$\begin{aligned} &\mathbb{P}(C_{n,12}(t_0) = 1)^{-2} \int_{-1}^1 \int_{-1}^1 K(u)K(v)T_{n,2}(u, v)dudv \\ &= \left[\int_{-1}^1 K(u)a_n(u)f_2(\theta_{0,n}, t_0 + uh)du \right]^2 \rightarrow f_2(\theta_0(t_0), t_0)^2, \end{aligned} \quad (4.16)$$

where, again, (2.10) and continuity of $f_2(\theta, t) = -\partial_{\theta^2}g(\theta, t)$ has been used. Furthermore, we have that

$$\begin{aligned} &\mathbb{P}(C_{n,12}(t_0) = 1)^{-2} \int_{-1}^1 \int_{-1}^1 K(u)K(v)T_{n,1}(u, v)dudv \\ &= \int_{-1}^1 \int_{-1}^1 K(u)K(v) \frac{\mathbb{P}(C_{n,ij}(t_0 + uh) = 1, C_{n,kl}(t_0 + vh) = 1)}{\mathbb{P}(C_{n,12}(t_0) = 1)^2} \\ &\quad \times (f_{n,1}(\theta_{0,n}, t_0 + uh, t_0 + vh | (i, j), (k, l)) - f_1(\theta_0(t_0), |\{i, j\} \cap \{k, l\}|)) dudv \\ &+ \int_{-1}^1 \int_{-1}^1 K(u)K(v) \frac{\mathbb{P}(C_{n,ij}(t_0 + uh) = 1, C_{n,kl}(t_0 + vh) = 1)}{\mathbb{P}(C_{n,12}(t_0) = 1)^2} \\ &\quad \times f_1(\theta_0(t_0), |\{i, j\} \cap \{k, l\}|) dudv \\ &\begin{cases} = o(n^2) & \text{for } |\{i, j\} \cap \{k, l\}| = 2 \\ = o(n) & \text{for } |\{i, j\} \cap \{k, l\}| = 1 \\ \rightarrow f_1(\theta_0(t_0), 0) = f_2(\theta_0(t_0), t_0)^2 & \text{for } |\{i, j\} \cap \{k, l\}| = 0 \end{cases} \end{aligned} \quad (4.17)$$

by Assumptions (2.11) and (2.17). From (4.16) and (4.17), we obtain (4.15). This shows (4.8).

For the proof of (4.9), we calculate a bound for the expectation of the absolute value of the third derivative of P_n . With $s = t_0 + uh$, it holds

$$\mathbb{E} \left(\sup_{k,l,r,\theta} \left| \frac{\partial^2}{\partial \theta_k \partial \theta_l} P_n^{(r)}(\theta) \right| \right)$$

$$\leq \frac{1}{\mathbb{P}(C_{n,12}(t_0) = 1)} \int_{-1}^1 K(u) \mathbb{P}(C_{n,12}(s) = 1) \mathbb{E} \left(\|Y_{n,12}(s)\|^3 e^{\tau Y_{n,12}(s)} \middle| C_{n,12}(s) = 1 \right) du,$$

where (2.6) has been used to get that the order of differentiation and integration can be interchanged and where Fubini could be used because all involved terms are non-negative. The upper bound for the expectation in the integral expression is bounded by Assumptions (2.6) and (2.10). This shows (4.9). \square

Lemma 4.5. *It holds that*

$$\begin{aligned} & \frac{1}{l_n h} \sum_{i,j=1}^n \int_0^T K\left(\frac{s-t_0}{h}\right) C_{n,ij}(t_0) \left[C_{n,ij}(s) Y_{n,ij}(s) \left(e^{\theta_0(s)^T Y_{n,ij}(s)} - e^{\theta_{0,n}^T Y_{n,ij}(s)} \right) \right. \\ & \left. - \partial_{\theta} g(\theta_{0,n}, s) \right] ds = o_P\left(\frac{1}{\sqrt{l_n h}}\right) \end{aligned} \quad (4.18)$$

and

$$\begin{aligned} & \frac{1}{l_n h} \sum_{i,j=1}^n \int_0^T K\left(\frac{s-t_0}{h}\right) (1 - C_{n,ij}(t_0)) C_{n,ij}(s) Y_{n,ij}(s) \left(e^{\theta_0(s)^T Y_{n,ij}(s)} - e^{\theta_{0,n}^T Y_{n,ij}(s)} \right) ds \\ & = o_P(h^2). \end{aligned} \quad (4.19)$$

Proof. We start by proving (4.19). Note that, for $U_h := [t_0 - h, t_0 + h]$, by an application of Taylor's Theorem, it holds that

$$\begin{aligned} & \sup_{s \in U_h} \left\| Y_{n,ij}(s) \left(e^{\theta_0(s)^T Y_{n,ij}(s)} - e^{\theta_{0,n}^T Y_{n,ij}(s)} \right) \right\| \\ & \leq \sup_{s \in U_h} \left\| Y_{n,ij}(s) Y_{n,ij}(s)^T \int_0^1 e^{[\theta_0(s) - \alpha(\theta_0(s) - \theta_{0,n})]^T Y_{n,ij}(s)} d\alpha \right\| \cdot \sup_{s \in U_h} \|\theta_0(s) - \theta_{0,n}\| \\ & \leq \sup_{s \in U_h} \|Y_{n,ij}(s)\|^2 e^{\tau \|Y_{n,ij}(s)\|} \cdot \sup_{s \in U_h} \|\theta_0(s) - \theta_{0,n}\|. \end{aligned} \quad (4.20)$$

For the proof of (4.19), we show that the expectation of the absolute value of the left hand side of (4.19) is $o(h^2)$ which yields the statement by Markov's Inequality. The expectation can be computed as follows

$$\begin{aligned} & \mathbb{E} \left\| \frac{1}{l_n h} \sum_{i,j=1}^n \int_0^T K\left(\frac{s-t_0}{h}\right) (1 - C_{n,ij}(t_0)) C_{n,ij}(s) Y_{n,ij}(s) \right. \\ & \quad \left. \times \left(e^{\theta_0(s)^T Y_{n,ij}(s)} - e^{\theta_{0,n}^T Y_{n,ij}(s)} \right) ds \right\| \\ & \leq \mathbb{E} \left(\int_0^T \frac{1}{h} K\left(\frac{s-t_0}{h}\right) \frac{(1 - C_{n,12}(t_0)) C_{n,12}(s)}{\mathbb{P}(C_{n,12}(t_0) = 1)} \right. \\ & \quad \left. \times \left\| Y_{n,12}(s) \left(e^{\theta_0(s)^T Y_{n,12}(s)} - e^{\theta_{0,n}^T Y_{n,12}(s)} \right) \right\| ds \right) \end{aligned}$$

$$\begin{aligned}
&\leq \int_0^T \frac{1}{h} K\left(\frac{s-t_0}{h}\right) \mathbb{E}\left(\frac{(1-C_{n,12}(t_0))C_{n,12}(s)}{\mathbb{P}(C_{n,12}(t_0)=1)} \|Y_{n,12}(s)\|^2 e^{\tau\|Y_{n,12}(s)\|}\right) ds \\
&\quad \times \sup_{s \in U_h} \|\theta_0(s) - \theta_{0,n}\| \\
&= \int_0^T \frac{1}{h} K\left(\frac{s-t_0}{h}\right) \frac{\mathbb{P}(C_{n,12}(s)=1)}{\mathbb{P}(C_{n,12}(t_0)=1)} \mathbb{E}\left((1-C_{n,12}(t_0))\|Y_{n,12}(s)\|^2\right. \\
&\quad \left. \times e^{\tau\|Y_{n,12}(s)\|} \Big| C_{n,12}(s)=1\right) ds \cdot \sup_{s \in U_h} \|\theta_0(s) - \theta_{0,n}\| \\
&= \int_0^T \frac{1}{h} K\left(\frac{s-t_0}{h}\right) \frac{\mathbb{P}(C_{n,12}(s)=1)}{\mathbb{P}(C_{n,12}(t_0)=1)} \cdot \frac{\mathbb{P}(C_{n,12}(t_0)=0, C_{n,12}(s)=1)}{\mathbb{P}(C_{n,12}(s)=1)} \\
&\quad \times \mathbb{E}\left(\|Y_{n,12}(s)\|^2 e^{\tau\|Y_{n,12}(s)\|} \Big| C_{n,12}(s)=1, C_{n,12}(t_0)=0\right) ds \\
&\quad \times \sup_{s \in U_h} \|\theta_0(s) - \theta_{0,n}\| \\
&\leq \int_0^T \frac{1}{h} K\left(\frac{s-t_0}{h}\right) \frac{\mathbb{P}(C_{n,12}(s)=1)}{\mathbb{P}(C_{n,12}(t_0)=1)} ds \\
&\quad \times \sup_{s \in U_h} \mathbb{E}\left(\|Y_{n,12}(s)\|^2 e^{\tau\|Y_{n,12}(s)\|} \Big| C_{n,12}(s)=1, C_{n,12}(t_0)=0\right) \\
&\quad \times \sup_{s \in U_h} \frac{\mathbb{P}(C_{n,12}(t_0)=0, C_{n,12}(s)=1)}{\mathbb{P}(C_{n,12}(s)=1)} \cdot \sup_{s \in U_h} \|\theta_0(s) - \theta_{0,n}\|,
\end{aligned}$$

where, in the third line, the previous inequality and Fubini was used, and where, in the fourth step, we use the definition of the conditional expectation.

By assumptions (2.10) and (2.8), respectively, the first two factors of the upper bound are bounded. The last two factors are of order $o(h)$ and $O(h)$, respectively. For former follows from (2.12), and the latter follows, because $\theta_{0,n} - \theta_0(t_0) = O(h^2)$, and $\sup_{s \in U_h} \|\theta_0(s) - \theta_0(t_0)\| = O(h)$. This concludes the proof of (4.19).

To prove (4.18), we have to show that

$$\frac{1}{\sqrt{lnh}} \sum_{i,j} \int_0^T K\left(\frac{s-t_0}{h}\right) C_{n,ij}(t_0) r_{n,ij}(s) ds = o_P(1),$$

where $r_{n,ij}(s)$ was defined in Assumption (A7). By an application of Markov's inequality, this holds if

$$\begin{aligned}
&\frac{h}{ln} \sum_{(i,j),(k,l)} \int_{-1}^1 \int_{-1}^1 K(u)K(v) \mathbb{P}(C_{n,ij}(t_0)=1, C_{n,kl}(t_0)=1) \\
&\quad \times \mathbb{E}(r_{n,ij}(t_0+uh)r_{n,kl}(t_0+vh) | C_{n,ij}(t_0)=1, C_{n,kl}(t_0)=1) dudv = o(1).
\end{aligned}$$

We show this similarly as in the proof of Lemma 4.4 by splitting the sum in three sums corresponding to $|\{i,j\} \cap \{k,l\}| = 2, 1, \text{ or } 0$. The corresponding sums have $O(n^2), O(n^3)$ and

$O(n^4)$ terms, respectively. Before going through these three cases, we note that equations (4.20) and (2.7) imply that $\sup_{u,v \in [-1,1]} \mathbb{E}(r_{n,ij}(t_0+uh)r_{n,kl}(t_0+vh) | C_{n,ij}(t_0) = 1, C_{n,kl}(t_0) = 1) = O(h^2)$. This rate holds for all (i, j) and (k, l) . Now we get for the sum over edges with $|\{i, j\} \cap \{k, l\}| = 2$ the bound

$$h \frac{\mathbb{P}(C_{n,12}(t_0) = 1)}{\mathbb{P}(C_{n,12}(t_0) = 1)} \int_{-1}^1 \int_{-1}^1 K(u)K(v)O(h^2)dudv = o(1).$$

For the sum over edges with $|\{i, j\} \cap \{k, l\}| = 1$, we get the following bound from (2.13)

$$nh\mathbb{P}(C_{n,12}(t_0) = 1) \frac{\mathbb{P}(C_{n,12}(t_0) = 1, C_{n,23}(t_0) = 1)}{\mathbb{P}(C_{n,12}(t_0) = 1)^2} O(h^2) = O(1) \cdot \frac{l_n}{n} O(h^3).$$

Observing that $\frac{l_n h^3}{n} = \frac{l_n^{3/5} (h^5)^{3/5} l_n^{2/5}}{n} = O\left(\frac{l_n^{2/5}}{n}\right) = O(n^{-1/5} P(C_{n,12}(t_0) = 1)^{2/5}) = o(1)$, the bound is of order $o(1)$.

By using (2.13) and (2.18), we get the following bound for the sum over edges with $|\{i, j\} \cap \{k, l\}| = 0$:

$$\begin{aligned} & l_n h \frac{\mathbb{P}(C_{n,12}(t_0) = 1, C_{n,34}(t_0) = 1)}{\mathbb{P}(C_{n,12}(t_0) = 1)^2} \\ & \int_{-1}^1 \int_{-1}^1 K(u)K(v) \mathbb{E}(r_{n,12}(t_0+uh)r_{n,34}(t_0+vh) | C_{n,12}(t_0) = 1, C_{n,34}(t_0) = 1) dudv \\ & = o(1). \end{aligned}$$

This concludes the proof of (4.18). □

Proposition 4.3. *With probability tending to one, the equation $P'_n(\theta) = 0$ (cf. equation (4.2)) has a solution $\tilde{\theta}_n(t_0)$, which has the property*

$$\tilde{\theta}_n(t_0) = \theta_{0,n} + o_P\left(\frac{1}{\sqrt{l_n h}}\right) + o_P(h^2).$$

To prove this proposition, we will make use of the following theorem, see Deimling (1985):

Theorem 4.4. (*Newton-Kantorovich Theorem*) *Let $R(x) = 0$ be a system of equations where $R : D_0 \subseteq \mathbb{R}^q \rightarrow \mathbb{R}$ is a function defined on D_0 . Let R be differentiable and denote by R' its first derivative. Assume that there is an x_0 such that all expressions in the following statements exist and such that the following statements are true*

1. $\|R'(x_0)^{-1}\| \leq B$,
2. $\|R'(x_0)^{-1}R(x_0)\| \leq \eta$,
3. $\|R'(x) - R'(y)\| \leq K\|x - y\|$ for all $x, y \in D_0$,

4. $r := BK\eta \leq \frac{1}{2}$ and $\Omega_* := \{x : \|x - x_0\| < 2\eta\} \subseteq D_0$.

Then there is $x^* \in \Omega_*$ with $R(x^*) = 0$ and

$$\|x^* - x_0\| \leq 2\eta \text{ and } \|x^* - (x_0 - R'(x_0)^{-1}R(x_0))\| \leq 2r\eta.$$

Proof of Proposition 4.3. We show that $P'_n(\theta)$ has a root by using Theorem 4.4. Lemma 4.4 gives that $P'_n(\theta_{0,n}) \xrightarrow{\mathbb{P}} 0$ and $P''_n(\theta_{0,n}) \xrightarrow{\mathbb{P}} -\Sigma$. Since Σ is invertible we also have that the sequence of random variables $B_n := \|P''_n(\theta_{0,n})^{-1}\|$ is well-defined (for large n) and that it is of order $O_P(1)$. Thus we also have $\eta_n := \|P''_n(\theta_{0,n})^{-1}P'_n(\theta_{0,n})\| = o_P(1)$. For the Lipschitz continuity of P''_n we bound the partial derivatives of P''_n by Lemma 4.4. Hence we conclude that every realisation of P''_n is Lipschitz continuous with (random) Lipschitz constant $K_n = O_P(1)$. Combining everything, we get that $r_n := B_n K_n \eta_n = o_P(1)$. Thus with probability tending to one we have $r_n \leq \frac{1}{2}$, and hence the Newton-Kantorovich Theorem tells us that with probability tending to one the equation $P'_n(\theta) = 0$ has a solution $\tilde{\theta}_n(t_0)$ with the property that

$$\|\tilde{\theta}_n(t_0) - \theta_{0,n}\| \leq 2\eta_n = o_P(1).$$

To prove the asserted rate, we have to investigate η_n further. We note first that since $P''_n(\theta_{0,n})^{-1}$ is stochastically bounded, the rate of η_n is determined by the rate with which $P'_n(\theta_{0,n})$ converges to zero. To find this rate we observe that every summand of $P'_n(\theta_{0,n})$ has expectation zero conditionally on $C_{n,ij}(s) = 1$:

$$\begin{aligned} & \int_0^T K \left(\frac{s-t_0}{h} \right) \mathbb{E} \left[C_{n,ij}(s) Y_{n,ij}(s) \left(e^{\theta_0(s)^T Y_{n,ij}(s)} - e^{\theta_{0,n}^T Y_{n,ij}(s)} \right) \middle| C_{n,ij}(s) = 1 \right] ds \\ &= \int_0^T K \left(\frac{s-t_0}{h} \right) \partial_{\theta} g(\theta_{0,n}, s) ds \\ &= 0 \end{aligned}$$

by the assumption that $\theta_{0,n}$ maximizes $\theta \mapsto \int_0^T K \left(\frac{s-t_0}{h} \right) g(\theta, s) ds$. So, in $P'_n(\theta_{0,n})$, we can subtract $C_{n,ij}(t_0) \int_0^T K \left(\frac{s-t_0}{h} \right) \partial_{\theta} g(\theta_{0,n}, s) ds$ from every summand without changing anything, i.e.,

$$\begin{aligned} P'_n(\theta_{0,n}) &= \frac{1}{l_n h} \sum_{i,j=1}^n \int_0^T K \left(\frac{s-t_0}{h} \right) \left[C_{n,ij}(s) Y_{n,ij}(s) \left(e^{\theta_0(s)^T Y_{n,ij}(s)} - e^{\theta_{0,n}^T Y_{n,ij}(s)} \right) \right. \\ &\quad \left. - C_{n,ij}(t_0) \partial_{\theta} g(\theta_{0,n}, s) \right] ds \\ &= \frac{1}{l_n h} \sum_{i,j=1}^n \int_0^T K \left(\frac{s-t_0}{h} \right) C_{n,ij}(t_0) \left[C_{n,ij}(s) Y_{n,ij}(s) \left(e^{\theta_0(s)^T Y_{n,ij}(s)} \right. \right. \\ &\quad \left. \left. - e^{\theta_{0,n}^T Y_{n,ij}(s)} \right) - \partial_{\theta} g(\theta_{0,n}, s) \right] ds \end{aligned}$$

$$\begin{aligned}
& + \frac{1}{l_n h} \sum_{i,j=1}^n \int_0^T K\left(\frac{s-t_0}{h}\right) (1 - C_{n,ij}(t_0)) C_{n,ij}(s) Y_{n,ij}(s) \\
& \quad \times \left(e^{\theta_0(s)^T Y_{n,ij}(s)} - e^{\theta_{0,n}^T Y_{n,ij}(s)} \right) ds.
\end{aligned}$$

By Lemma 4.5, this term is $o_P\left(\frac{1}{\sqrt{l_n h}}\right) + o_P(h^2)$, which concludes the proof of Proposition 4.3. \square

Lemma 4.6. For $k, l \in \{1, \dots, q\}$, we have that

$$\frac{1}{l_n h} \sum_{i,j=1}^n \int_0^T K\left(\frac{s-t_0}{h}\right)^2 Y_{n,ij}^{(l)}(s) Y_{n,ij}^{(k)}(s) C_{n,ij}(s) \exp(\theta_0(s)^T Y_{n,ij}(s)) ds \xrightarrow{\mathbb{P}} \int_{-1}^1 K(u)^2 du \Sigma_{k,l} \quad (4.21)$$

and

$$\begin{aligned}
& \frac{1}{l_n h} \sum_{i,j=1}^n \int_0^T K\left(\frac{s-t_0}{h}\right)^2 \|Y_{n,ij}(s)\|^2 \mathbb{1}\left(\frac{1}{\sqrt{l_n h}} \left\| K\left(\frac{s-t_0}{h}\right) Y_{n,ij}(s) \right\| > \epsilon\right) \\
& \quad \times C_{n,ij}(s) \exp(\theta_0(s)^T Y_{n,ij}(s)) ds \xrightarrow{\mathbb{P}} 0.
\end{aligned} \quad (4.22)$$

Moreover, it holds that

$$\frac{1}{l_n} \partial_{\theta}^2 \ell(\tilde{\theta}_n(t_0), t_0) = P_n''(\tilde{\theta}_n(t_0)) \xrightarrow{\mathbb{P}} -\Sigma. \quad (4.23)$$

Proof. The proof of (4.21) follows by using similar arguments as in the proof of Lemma 4.4, with $\theta_{0,n}$ replaced by $\theta_0(s)$, and with K replaced by K^2 .

For the proof of claim (4.22), we calculate the expectation of the left hand side of (4.22). Because the integrand is positive, we can apply Fubini, and we get that the expectation is equal to

$$\begin{aligned}
& \int_0^T \mathbb{E} \left[\mathbb{1}\left(\frac{1}{\sqrt{l_n h}} \left\| K\left(\frac{s-t_0}{h}\right) Y_{n,12}(s) \right\| > \epsilon\right) \|Y_{n,12}(s)\|^2 \right. \\
& \quad \left. \times \exp\left(\theta_0(s)^T Y_{n,12}(s)\right) \Big| C_{n,12}(s) = 1 \right] \frac{1}{h} K\left(\frac{s-t_0}{h}\right)^2 \frac{\mathbb{P}(C_{n,12}(s) = 1)}{\mathbb{P}(C_{n,12}(t_0) = 1)} ds \\
& \leq \frac{1}{\epsilon} \cdot \frac{1}{\sqrt{l_n h}} \int_{-1}^1 K^3(u) \frac{\mathbb{P}(C_{n,12}(t_0 + uh) = 1)}{\mathbb{P}(C_{n,12}(t_0) = 1)} \\
& \quad \mathbb{E} \left(\|Y_{n,12}(t_0 + uh)\|^3 e^{\tau \|Y_{n,12}(t_0 + uh)\|} \Big| C_{n,12}(t_0 + uh) = 1 \right) du \\
& = O\left(\frac{1}{\sqrt{l_n h}}\right) = o(1).
\end{aligned}$$

Here we use (2.10), $\max_{-1 \leq u \leq 1} K(u) < \infty$ and (2.9). This shows (4.22).

To see (4.23), we show that

$$P_n''(\theta_{0,n}) - P_n''(\tilde{\theta}_n(t_0)) = o_P(1). \quad (4.24)$$

This then implies (4.23) because of (4.8).

By using exactly the same arguments as in the proof of Lemma 4.5, we obtain

$$e^{\theta_{0,n}^T Y_{n,ij}(s)} - e^{\tilde{\theta}_n(t_0)^T Y_{n,ij}(s)} \leq \|Y_{n,ij}(s)\| e^{\tau \|Y_{n,ij}(s)\|} \cdot \|\theta_{0,n} - \tilde{\theta}_n(t_0)\|.$$

This gives

$$\begin{aligned} & P_n''(\theta_{0,n}) - P_n''(\tilde{\theta}_n(t_0)) \\ &= \frac{1}{l_n h} \sum_{i,j=1}^n \int_0^T K\left(\frac{s-t_0}{h}\right) C_{n,ij}(s) Y_{n,ij}(s) Y_{n,ij}(s)^T \left(e^{\tilde{\theta}_n(t_0)^T Y_{n,ij}(s)} - e^{\theta_{0,n}^T Y_{n,ij}(s)} \right) ds \\ &\leq \frac{1}{l_n h} \sum_{i,j=1}^n \int_0^T K\left(\frac{s-t_0}{h}\right) C_{n,ij}(s) \|Y_{n,ij}(s)\|^3 e^{\tau \|Y_{n,ij}(s)\|} ds \times \|\theta_{0,n} - \tilde{\theta}_n(t_0)\|. \end{aligned}$$

The expectation of the first factor is bounded because of assumptions (2.10) and (2.9). Furthermore, the second term is of order $o_P(1)$ by Proposition 4.3. Thus, the product is of order $o_P(1)$. This shows (4.24) and concludes the proof of (4.23). \square

Proposition 4.5. *With probability tending to one, $\partial_{\theta} \ell_T(\theta, t_0) = 0$ has a solution $\hat{\theta}_n(t_0)$, and*

$$\sqrt{l_n h} \cdot (\hat{\theta}_n(t_0) - \tilde{\theta}_n(t_0)) \xrightarrow{d} N\left(0, \int_{-1}^1 K^2(u) du \Sigma^{-1}\right).$$

Proof of Proposition 4.5. The proof is based on modifications of arguments used in the asymptotic analysis of parametric counting process models, see e.g. the proof of Theorem VI.1.1 on p. 422 in Andersen et al. (1993). Define

$$U^l(\theta) := h \partial_{\theta_l} \ell_T(\theta, t_0), \quad l = 1, \dots, q,$$

and let $U_t^l(\theta)$ be defined as $U^l(\theta)$, but with t being the upper limit of the integral in (2.5), (i.e., $U^l(\theta) = U_T^l(\theta)$). Furthermore, we write $U(\theta) = (U^1(\theta), \dots, U^q(\theta))$, and the vector $U_t(\theta)$ is defined analogously. In the first step of the proof, we will show that

$$\frac{1}{\sqrt{l_n h}} U_T(\tilde{\theta}_n(t_0)) \xrightarrow{d} N\left(0, \int_{-1}^1 K^2(u) du \Sigma\right). \quad (4.25)$$

For the local, square integrable martingale $M_{n,ij}$ defined in (4.1), it holds that $M_{n,ij}$ and $M_{n,i'j'}$ are orthogonal, meaning that $\langle M_{n,ij}, M_{n,i'j'} \rangle_t = 0$ if $(i, j) \neq (i', j')$, i.e. the

predictable covariation process is equal to zero. For the predictable variation process of $M_{n,ij}$, we have

$$\langle M_{n,ij} \rangle_t = \int_0^t C_{n,ij}(s) \exp(\theta_0(s)^T Y_{n,ij}(s)) ds. \quad (4.26)$$

By definition of $\tilde{\theta}_n(t_0)$, see the statement of Proposition 4.3, we have that

$$\begin{aligned} & U_t^l(\tilde{\theta}_n(t_0)) \\ = & \sum_{i,j=1}^n \int_0^t K\left(\frac{s-t_0}{h}\right) Y_{n,ij}^{(l)}(s) dN_{n,ij}(s) \\ & - \int_0^t K\left(\frac{s-t_0}{h}\right) C_{n,ij}(s) Y_{n,ij}^{(l)}(s) \exp(\tilde{\theta}_n(t_0)^T Y_{n,ij}(s)) ds \\ = & \sum_{i,j=1}^n \int_0^t K\left(\frac{s-t_0}{h}\right) Y_{n,ij}^{(l)}(s) dM_{n,ij}(s) \\ & + \int_0^t K\left(\frac{s-t_0}{h}\right) C_{n,ij}(s) Y_{n,ij}^{(l)}(s) \left(\exp(\theta_0(s)^T Y_{n,ij}(s)) - \exp(\tilde{\theta}_n(t_0)^T Y_{n,ij}(s)) \right) ds \\ = & \sum_{i,j=1}^n \int_0^t K\left(\frac{s-t_0}{h}\right) Y_{n,ij}^{(l)}(s) dM_{n,ij}(s). \end{aligned} \quad (4.27)$$

So $\tilde{\theta}_n(t_0)$ was chosen such that the non-martingale part of $\partial_\theta \ell(\tilde{\theta}_n(t_0), t_0)$ vanishes. Now, we want to apply Rebolledo's Martingale Convergence Theorem, see e.g. Theorem II.5.1 in Andersen et al.(1993). This theorem implies (4.25), provided a Lindeberg condition (4.22) holds, and

$$\left\langle \frac{1}{\sqrt{l_n h}} U_t^k(\tilde{\theta}_n(t_0)), \frac{1}{\sqrt{l_n h}} U_t^l(\tilde{\theta}_n(t_0)) \right\rangle_T \xrightarrow{\mathbb{P}} \int_{-1}^1 K^2(u) du \Sigma_{kl}(t_0). \quad (4.28)$$

To verify (4.28), first note that (4.26) and (4.21) imply finiteness of

$$\frac{1}{l_n h} \sum_{i,j=1}^n \int_0^t K\left(\frac{s-t_0}{h}\right)^2 \left(Y_{n,ij}^{(l)}(s) \right)^2 d\langle M_{n,ij} \rangle_s,$$

with probability tending to one. Note that Lemma 4.6 is formulated with $t = T$, but the integral is finite also for $t < T$ simply because the integrand is non-negative. From now on we assume the above integral is finite. The process

$$\frac{1}{\sqrt{l_n h}} \sum_{i,j=1}^n \int_0^t K\left(\frac{s-t_0}{h}\right) Y_{n,ij}^{(l)}(s) dM_{n,ij}(s)$$

is a local square integrable martingale, see e.g. Theorem II.3.1 on p.71 in Andersen et al.(1993). Since the martingales $M_{n,ij}$ are orthogonal, and by using Lemma 4.6, the predictable covariation satisfies

$$\left\langle \frac{1}{\sqrt{l_n h}} U_t^k(\tilde{\theta}_n(t_0)), \frac{1}{\sqrt{l_n h}} U_t^l(\tilde{\theta}_n(t_0)) \right\rangle_T$$

$$\begin{aligned}
&= \frac{1}{l_n h} \sum_{i,j=1}^n \int_0^T K \left(\frac{s-t_0}{h} \right)^2 Y_{n,ij}^{(k)}(s) Y_{n,ij}^{(l)}(s) C_{n,ij}(s) \exp(\theta_0(s)^T Y_{n,ij}(s)) ds \\
&\xrightarrow{\mathbb{P}} \int_{-1}^1 K^2(u) du \Sigma_{kl}(t_0).
\end{aligned}$$

This shows (4.28), and concludes the proof of (4.25).

We now show that

$$\|\sqrt{l_n h} \cdot (\tilde{\theta}_n(t_0) - \hat{\theta}_n(t_0)) - \sqrt{l_n h} Z_n\| \xrightarrow{\mathbb{P}} 0, \quad (4.29)$$

where

$$Z_n = P_n''(\tilde{\theta}_n(t_0))^{-1} \frac{1}{l_n h} U(\tilde{\theta}_n(t_0)).$$

We want to apply the Newton-Kantorovich Theorem 4.4 with $R(\theta) := R_n(\theta) := \frac{1}{l_n h} U(\theta)$ and $x_0 := \tilde{\theta}_n(t_0)$. To this end, define

$$B_n := \|R_n'(\tilde{\theta}_n(t_0))^{-1}\| = \left\| P_n''(\tilde{\theta}_n(t_0))^{-1} \right\|.$$

From Lemma 4.6, we know that $P_n''(\tilde{\theta}_n(t_0))$ converges and is invertible for n large enough, and thus $B_n = O_P(1)$. Now let

$$\eta_n := \|R_n'(\tilde{\theta}_n(t_0))^{-1} R_n(\tilde{\theta}_n(t_0))\| = \|Z_n\|.$$

Results (4.23) and (4.25) imply that $\eta_n = o_P(1)$. Next, notice that P_n'' has a Lipschitz constant K_n that is bounded by the maximum of the third derivative of P_n . According to (4.9), this maximum is bounded, and we obtain $K_n = O_P(1)$. Hence, $r_n = B_n K_n \eta_n = o_P(1)$. Now, Theorem 4.4 implies that, with probability converging to one, there is $\hat{\theta}_n(t_0)$ such that $U(\hat{\theta}_n(t_0)) = 0$ and

$$\|\hat{\theta}_n(t_0) - \tilde{\theta}_n(t_0)\| \leq 2\eta_n \xrightarrow{\mathbb{P}} 0.$$

To obtain the asymptotic distribution of $\hat{\theta}_n(t_0)$, we note that, by (4.25) and (4.23),

$$\sqrt{l_n h} \cdot Z_n \xrightarrow{d} N(0, \int_{-1}^1 K^2(u) du \Sigma^{-1}). \quad (4.30)$$

Thus it holds that $\sqrt{l_n h} \cdot Z_n = O_P(1)$, and as a consequence we get $\sqrt{l_n h} \cdot \eta_n = O_P(1)$. Using the second statement of the Newton-Kantorovich Theorem 4.4, we obtain

$$\|\sqrt{l_n h} \cdot (\tilde{\theta}_n(t_0) - \hat{\theta}_n(t_0)) - \sqrt{l_n h} Z_n\| \leq \sqrt{l_n h} \cdot 2r_n \eta_n = o_P(1).$$

Thus $\sqrt{l_n h} \cdot (\tilde{\theta}_n(t_0) - \hat{\theta}_n(t_0))$ and $\sqrt{l_n h} \cdot Z_n$ have the same limit distribution. Because of (4.30) this implies the statement of the proposition. \square

PROOF OF THEOREM 2.1 Combining Propositions 4.3 and 4.5, and applying Slutsky's Lemma, we obtain

$$\sqrt{l_n h} \left(\hat{\theta}_n(t_0) - \theta_{0,n}(t_0) \right) \rightarrow N \left(0, \int_{-1}^1 K^2(u) du \Sigma^{-1} A \Sigma^{-1} \right).$$

With Proposition 4.2 this gives (2.19).

5 Acknowledgement

The authors acknowledge support by the state of Baden-Württemberg through bwHPC and the German Research Foundation (DFG) through grant INST 35/1134-1 FUGG. Research of Alexander Kreiß and Enno Mammen was supported by Deutsche Forschungsgemeinschaft through the Research Training Group RTG 1953

References

- [1] Ahmed, A. and Xing, E.P. (2009): Recovering time-varying networks of dependencies in social and biological studies. *Proc. Nat. Acad. Sciences*, **107**, 11878-11883.
- [2] Andersen, P.K., Borgan, O., Gill, R.D., Keiding, N. (1993): *Statistical models based on counting processes*. Springer, New York
- [3] Backstrom, L. and Leskovec, J. (2011): Supervised random walks: predicting and recommending links in social networks. In *Proceedings of the fourth ACM international conference on Web search and data mining, WSDM '11*, 635-644.
- [4] Butts, C.T. (2008): A relational event framework for social action. *Sociol. Methodol.*, **38**, 155-200.
- [5] Deimling, K. (1985): *Nonlinear Functional Analysis*. Springer, Berlin.
- [6] Durante, D. and Dunson D. B. (2014): Nonparametric Bayes dynamic modelling of relational data. *Biometrika*, **101**, 883-898.
- [7] Foulds, J. R., DuBois, C., Asuncion, A. U., Butts, C. T., and Smyth, P. (2011): A dynamic relational infinite feature model for longitudinal social networks. In *Proceedings of the 14th International Conference on Artificial Intelligence and Statistics*, 287-295.
- [8] Goldenberg, A., Zheng, A.X., Fienberg, S.E. and Airoldi, E.M. (2010): A survey of statistical network models. *Foundations and Trends in Machine Learning* **2**, 129-233.
- [9] Guo, F., Hanneke, S., Fu, W. and Xing, E. P. (2007): Recovering temporally rewiring networks: A model-based approach. In *Proceedings of the 24th International Conference on Machine Learning*, 321-328. ACM Press, New York.

- [10] Hanneke, S., Fu, W. and Xing, E.P. (2010): Discrete temporal models of social networks. *Electronic J. Statist.* **4**, 585-605.
- [11] Hart, J. and YI, S. (1998): One-sided cross-validation. *J. Am. Statist. Assoc.* **93**, 620-631.
- [12] Ho, Q. Song, L. and Xing, E. P. (2011): Evolving cluster mixed-membership block-model for time-varying networks. In *JMLR Workshop and Conference Proceedings Volume 15: AISTATS 2011*, 342-350.
- [13] Ishiguro, K., Iwata, T., Ueda, N., Tenenbaum, J. (2010): Dynamic Infinite Relational Model for Time-varying Relational Data Analysis. In *Advances in Neural Information Processing Systems 23*, 919-927.
- [14] Jackson, M. O. (2008): *Social and Economic Networks*. Princeton University Press, Princeton and Oxford
- [15] Katz, L. and Proctor, C.H. (1959): The concept of configuration of interpersonal relations in groups as a time-dependent process. *Psychometrika*, **24**, 317- 327.
- [16] Kim, K. and Leskovec, J. (2013): Nonparametric multi-group membership model for dynamic networks. In *Advances in Neural Information Processing Systems 25*, 1385-1393.
- [17] Kolaczyk, E. D. (2009): *Statistical Analysis of Network Data: Methods and Models*. Springer, New York.
- [18] Kolar, M. and Xing, E.P. (2009): Sparsistent Estimation Of Time-Varying Markov Random Fields. *arXiv:0907.2337v2*
- [19] Krivitsky, P.N. (2012): Modeling of Dynamic Networks based on Egocentric Data with Durational Information. Pennsylvania State University Department of Statistics, Technical report (2012-01);
<http://stat.psu.edu/research/technical-reports/2012-technical-reports>
- [20] Krivitsky, P.N. and Handcock, M.S. (2014). A separable model for dynamic networks. *J. Royal Statist. Soc. Ser. B* **76**, 29-46.
- [21] Lee, N. H. and Priebe C. E. (2011): A latent process model for time series of attributed random graphs. *Statist. Inf. Stochastic Proc.*, **14**, 231- 253.
- [22] Leenders, R.Th. A.J. (1995): Models for network dynamics: A Markovian framework. *J. Math. Sociology* **20**, 1 - 20.
- [23] Liben-Nowell, D., Kleinberg, J. (2003): The Link Prediction Problem for Social Networks. In *Proceedings of the Twelfth International Conference on Information and Knowledge Management*, 556-559.

- [24] Liben-Nowell, D. and Kleinberg, J. (2007): The link-prediction problem for social networks. *J. Amer. Soc. Information Science Technology*, **58**, 1019-1031.
- [25] Mammen, E., Martinez-Miranda, M.D., Nielsen, J.P., Sperlich, S. (2011): Do-Validation for Kernel Density Estimation. *J. Am. Statist. Assoc.*, **106:494**, 651-660
- [26] Perry, P.O. and Wolfe, P.J. (2013): Point process modelling for directed interaction networks. *J. Royal Statist. Soc. Ser. B*, **75**, 821-849
- [27] Sarkar, P. and Moore, A. (2006): Dynamic social network analysis using latent space models. *SIGKDD Explor. Newsl.* **7**, 31-40.
- [28] Sarkar, P., Siddiq, S. M., and Gordon, G. J. (2007): A latent space approach to dynamic embedding of co-occurrence data. In *Proceedings of the 11th International Conference on Artificial Intelligence and Statistics*, 420-427.
- [29] Sewell, D.K. and Chen, Y. (2015): Latent space models for dynamic networks. *J. Amer. Statist. Assoc.*, DOI: 10.1080/01621459.2014.988214
- [30] Snijders, T.A.B. (1996): Stochastic actor-oriented models for network change. *J. Math. Sociology*, **21**, 149-172.
- [31] Snijders, T.A.B. (2001): The Statistical Evaluation of Social Network Dynamics. *Sociological Methodology*, **31**, 361-395.
- [32] Snijders, T. A. B., van de Bunt, G.G., and Steglich, C.E.G. (2010): Introduction to stochastic actor-based models for network dynamics. *Social Networks* **32**, 44-60.
- [33] Wasserman, S. (1980): Analyzing social networks as stochastic processes. *J. Amer. Statist. Assoc.*, **75**, 280-294.
- [34] Wasserman, S. and Faust, K. (1994). *Social Network Analysis: Methods and Applications*. Cambridge University Press.
- [35] Xing, E.P., Fu, W. and Song, L. (2012): A state-space mixed membership blockmodel for dynamic network tomography. *Ann. Appl. Statist.*, **4**, 535 - 566.
- [36] Xu, K.S. and Hero, A. O. (2014): Dynamic stochastic block-models for time-evolving social networks. *IEEE J. Select. Topics Signal Proc*, **8**, 552-562.
- [37] Xu, K.S. (2015): Stochastic Block Transition Models for Dynamic Networks. In *JMLR Workshop and Conference Proceedings, Volume 38*, 1079-1087.
- [38] Zafarani, R., Abbasi, M. A., Liu, H. (2014): *Social Media Mining*. Cambridge University Press
- [39] Zhou, S., Lafferty, J. and Wasserman, L. (2008): Time varying undirected graphs. In *Conference on Learning Theory* (R. A. Servedio and T. Zhang, eds.), 455-466. Omnipress, Madison, WI.

6 Supplementary material for the paper: "Nonparametric inference for continuous-time event counting and link-based dynamic network models" by Alexander Kreiß, Enno Mammen and Wolfgang Polonik.

6.1 Simulations of degree distributions, cluster coefficients and diameters.

Here we report additional simulations of degree distributions, cluster coefficients and diameters. In Section 3, we have presented results for the degree distribution of networks based on the Washington DC bikeshare activity on 7th December 2012. In this section, we will consider the days 18th April 2014 and 10th July 2015, and also compare diameters and clustering coefficients of the simulated and observed networks. As above, using the corresponding estimated parameter value for each of these days, we compute 3840 predictions and compared them with the observed values. The *diameter* of a network is the longest amongst the shortest path between two vertices in the network. Typically, in observed networks the diameter is much smaller than the number of vertices (cf. Jackson, 2008). The *clustering coefficient* is the number of complete triangles (triples of vertices which are completely connected) divided by the number of incomplete triangles (triples of vertices with at least two edges). Note that every complete triangle is also incomplete, hence the clustering coefficient is between zero and one. The clustering coefficient can be understood as the empirical probability that vertices are connected given that there is a third vertex to which both are connected. It has been reported (cf. Jackson, 2008), that in observed networks this number is usually significantly higher than in an Erdős-Rényi network, where the presence of edges are i.i.d. random variables.

Our question here is, *Does a network which was simulated by our model look like the observed network?* or in other words *Could one believe that the observed network is a realization of our model?* To answer this, we consider the three network characteristics mentioned above, and empirically and visually compare the simulated results to the observed data. The heuristic justification underlying this approach is, that, if considered jointly, these three characteristics are able to discriminate between a range of different types of networks (see also Jackson, 2008 and Zafarani et al., 2014)

We start by presenting results for diameter and clustering coefficient on 7th of December 2012. As described in Section 3, where the degree distribution was discussed, we divide the edges between bike stations in six regimes by considering tour frequencies between the stations on the day. Figure 6 shows the histograms of the simulated diameter in the different regimes. We see that, in 6e (as before in Figure 4e), the simulation and the reality appear to coincide nicely. In other words, for a moderate number of tours our model seems to fit well. It is interesting to note that our model performs differently in the different regimes suggesting that edges with different activity have to be modelled differently. Finally, in

Figure 7, we see the histograms of the simulated clustering coefficients. The true value in the corresponding regime is shown in the titles of the plots. Overall, the performance appears reasonable. In particular, in Figure 7d the histogram is nicely centered around the true value. Interestingly, the performance in the fifth regime ($l_1 = 5$ and $l_2 = 12$), shown in Figure 7e, is not as good as the others. One explanation for this might be that here different covariates are needed.

In Figure 14a we see one simulated graph compared to the true graph. The colour of the edges determine how many tours happened relative the the other edges: The lowest 25% of the edges are coloured green, the next 25% yellow, then orange and the highest 25% of edges are coloured red. Due to the integral value of the activity it is not the case that exactly 25% of the edges are green and so on. The size of the vertices is relative to their degree. We see that the model is able to find the *important* (i.e. high degree) vertices. For the edges we see that some red edges are at wrong places. But generally the vertices with high profile edges are recognized. The remaining graphs in Figure 14 show the same comparison for the two other dates under consideration. And we see that the results are similar.

Figures 8 till 13 show the results of the corresponding simulations for the other two dates. Overall the results are similar. It should be pointed out that even though the model is not able to reproduce every feature perfectly accurate, the simulated networks are still very close to the true observation. This becomes more obvious if we remind ourselves that only six parameters were used.

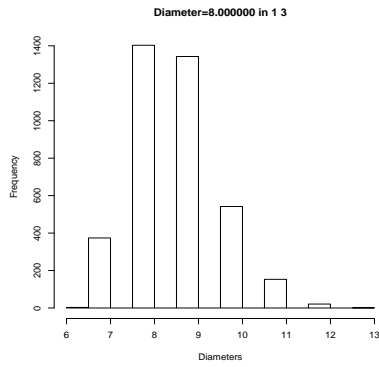
6.2 Bandwidth choice

Under our assumptions that the covariates stay constant over the day, it makes sense to consider only integral bandwidth lengths (for us one day has length one). In order to choose the bandwidth, we apply a one-sided cross validation (cf. Hart and Yi, 1998 and Mammen et al., 2011) approach which was shortly motivated in Section 3 and which we now describe in detail.

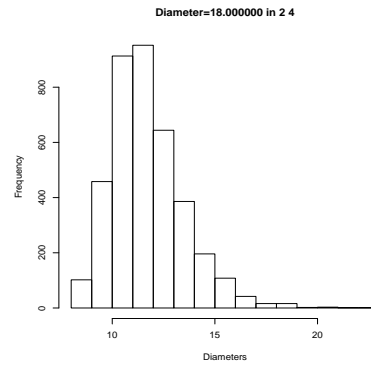
Let K and L be kernels fulfilling the assumptions in the paper and denote by $\hat{\theta}_K(t_0)$ and $\hat{\theta}_L(t_0)$ the maximum likelihood estimators using K and L respectively. Then, by Theorem 2.1, we get that asymptotically the bias and the variance of the estimators can be written as

$$\begin{aligned} \text{bias}(\hat{\theta}_K) &= h^2 \int_{-1}^1 K(u)u^2 du \cdot C_1 \\ \text{var}(\hat{\theta}_L) &= \frac{1}{l_n h} \int_{-1}^1 K(u)^2 du \cdot C_2 \end{aligned}$$

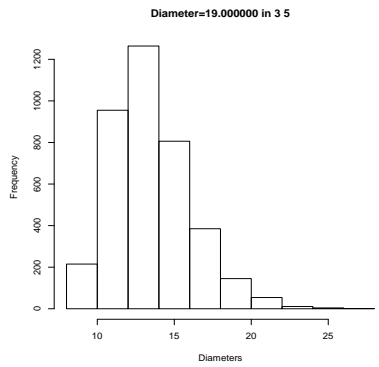
where the constants C_1 and C_2 depend on the true parameter curve θ_0 and the time t_0 but not on the kernel. Hence, the corresponding expressions for $\hat{\theta}_L(t_0)$ can be found, just by replacing every K with an L . The decomposition of the asymptotic mean squared error in



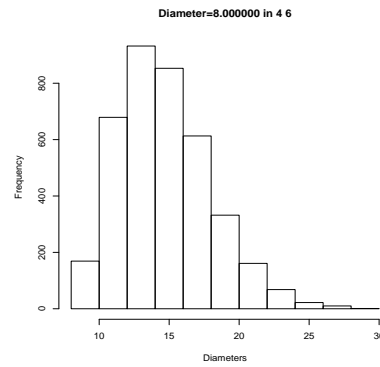
(a) Only edges with tour frequency between one and three



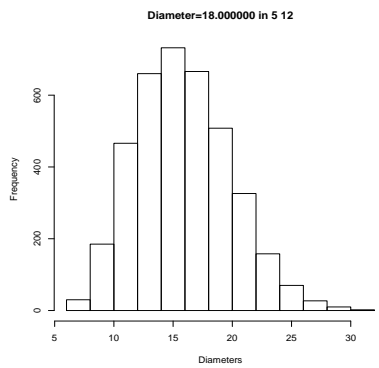
(b) Only edges with tour frequency between two and four



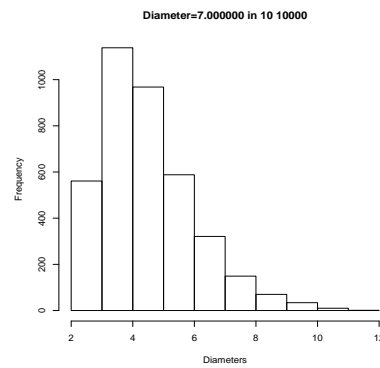
(c) Only edges with tour frequency between three and five



(d) Only edges with tour frequency between four and six

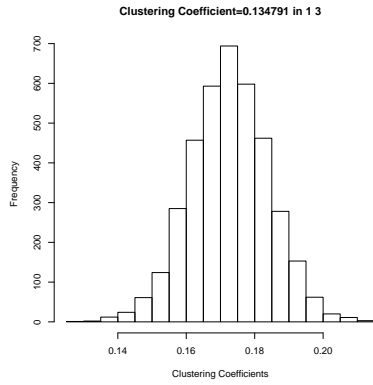


(e) Only edges with tour frequency between five and twelve

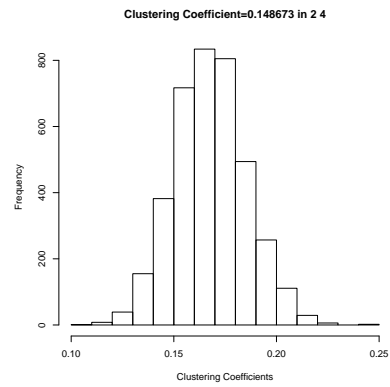


(f) Only edges with tour frequency larger than ten

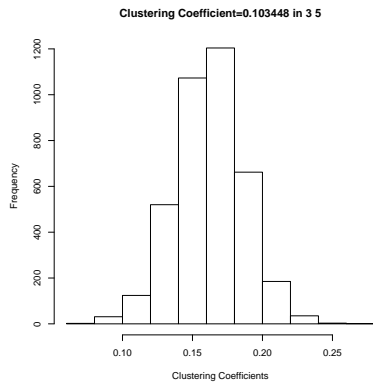
Figure 6: Histograms of diameters of the graphs which arise by taking different edges into account (see individual caption) from simulations for 7th December 2012. In the title of the plot the observed value is shown.



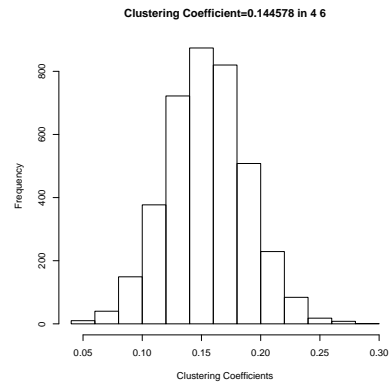
(a) Only edges with tour frequency between one and three



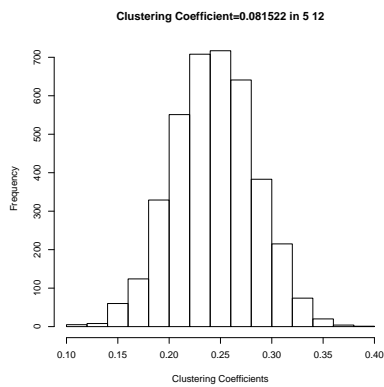
(b) Only edges with tour frequency between two and four



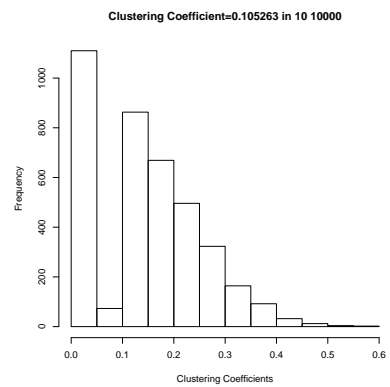
(c) Only edges with tour frequency between three and five



(d) Only edges with tour frequency between four and six

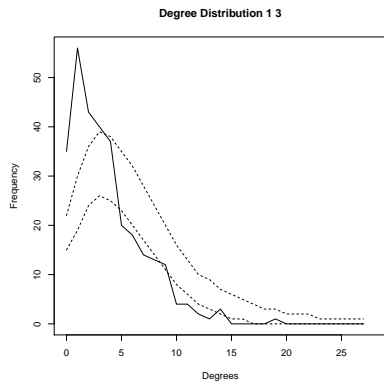


(e) Only edges with tour frequency between five and twelve

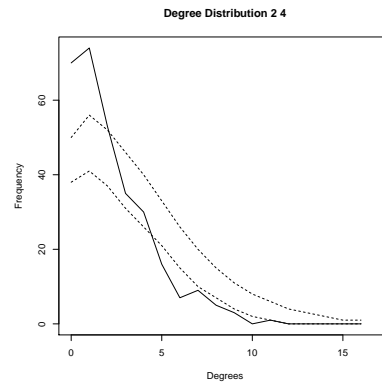


(f) Only edges with tour frequency larger than ten

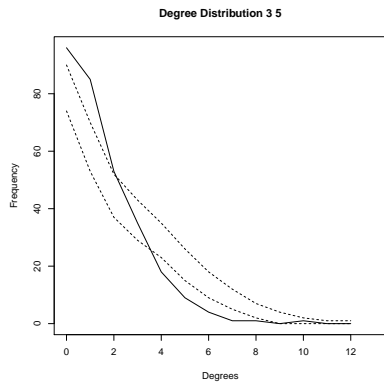
Figure 7: Histograms of clustering coefficients of the graphs which arise by taking different edges into account (see individual caption) from simulations for 7th December 2012. In the title of the plot the observed value is shown.



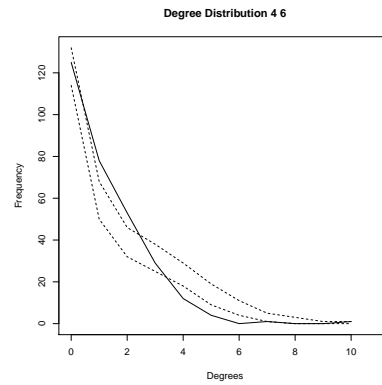
(a) Only edges with four frequency between one and three



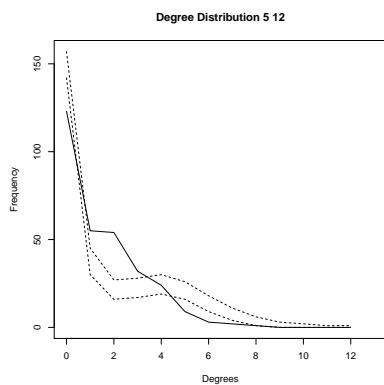
(b) Only edges with four frequency between two and four



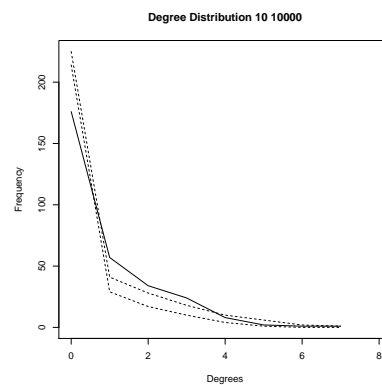
(c) Only edges with four frequency between three and five



(d) Only edges with four frequency between four and six

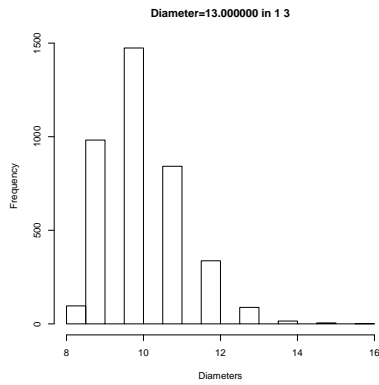


(e) Only edges with four frequency between five and twelve

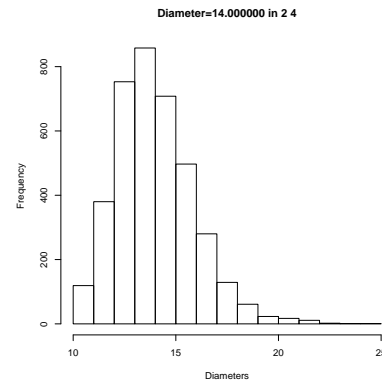


(f) Only edges with four frequency between larger than ten

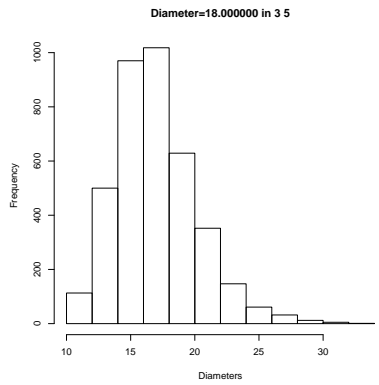
Figure 8: Degree distributions of the graphs which arise by taking different edges into account (see individual caption) from simulations for 18th April 2014. Dotted lines show 10% and 90% quantiles of simulations and solid line shows true distributions.



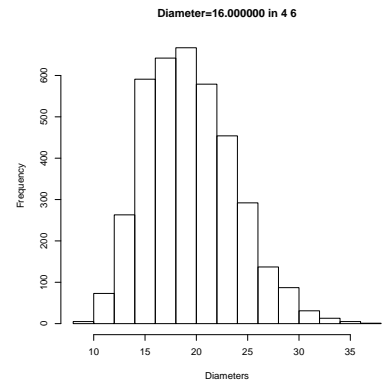
(a) Only edges with four frequency between one to three



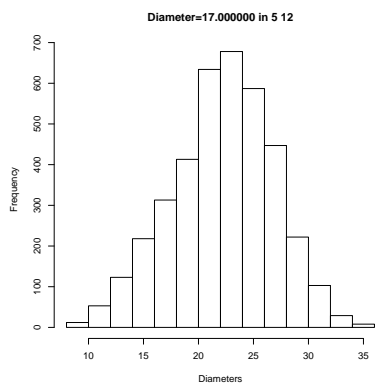
(b) Only edges with four frequency between two to four



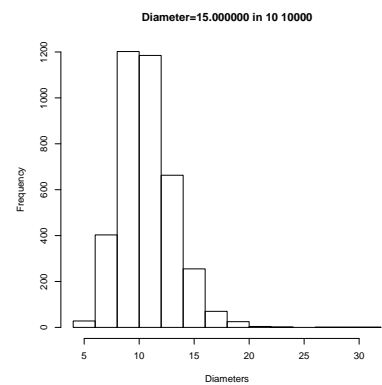
(c) Only edges with four frequency between three to five



(d) Only edges with four frequency between four to six

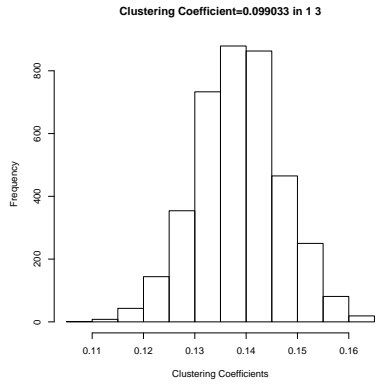


(e) Only edges with four frequency between five to twelve

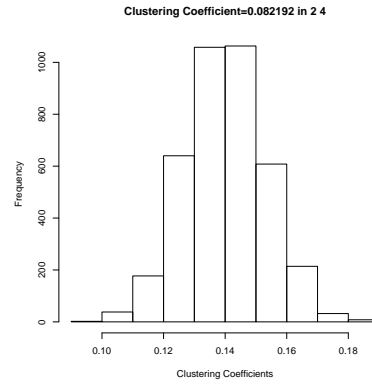


(f) Only edges with four frequency more than ten

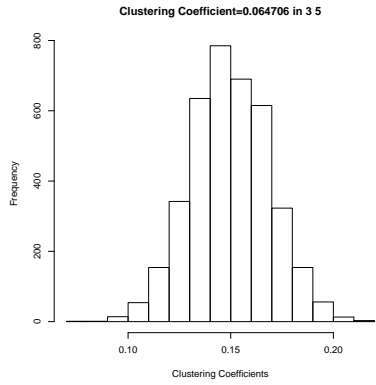
Figure 9: Histograms of diameters of the graphs which arise by taking different edges into account (see individual caption) from simulations for 18th April 2014. In the title of the plot the observed value is shown.



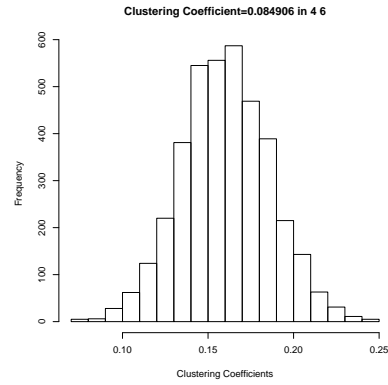
(a) Only edges with four frequency between one to three



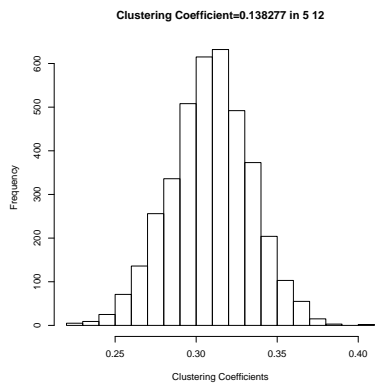
(b) Only edges with four frequency between two to four



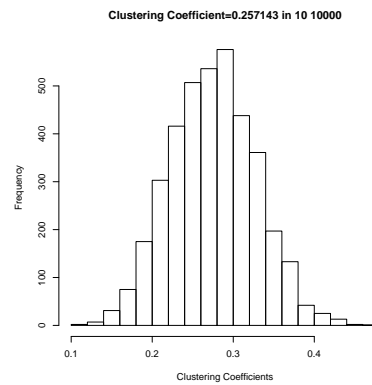
(c) Only edges with four frequency between three to five



(d) Only edges with four frequency between four to six

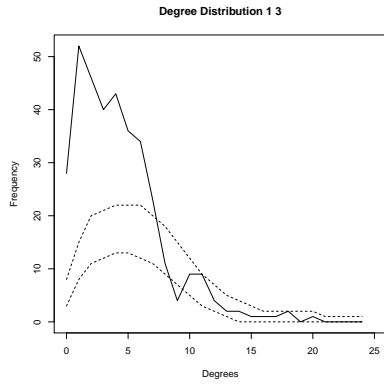


(e) Only edges with four frequency between five to twelve

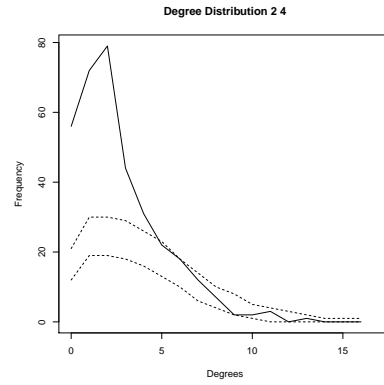


(f) Only edges with four frequency more than ten

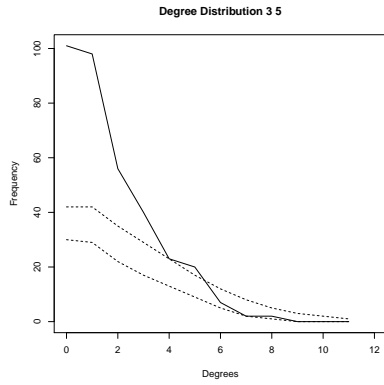
Figure 10: Histograms of clustering coefficients of the graphs which arise by taking different edges into account (see individual caption) from simulations for 18th April 2014. In the title of the plot the observed value is shown.



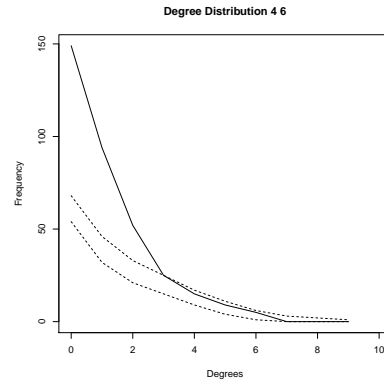
(a) Only edges with tour frequency between one to three



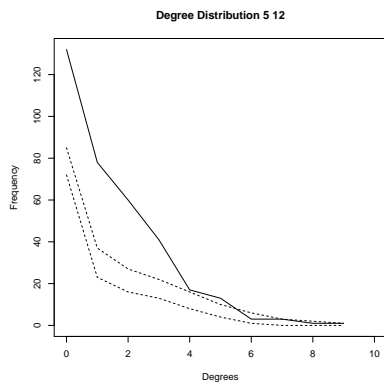
(b) Only edges with tour frequency between two to four



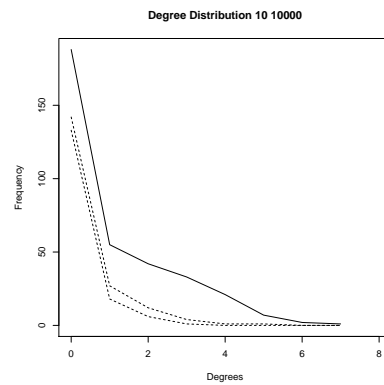
(c) Only edges with tour frequency between three to five



(d) Only edges with tour frequency between four to six

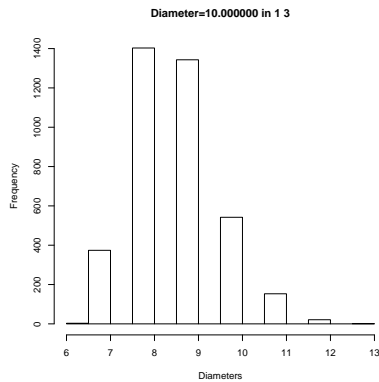


(e) Only edges with tour frequency between five to twelve

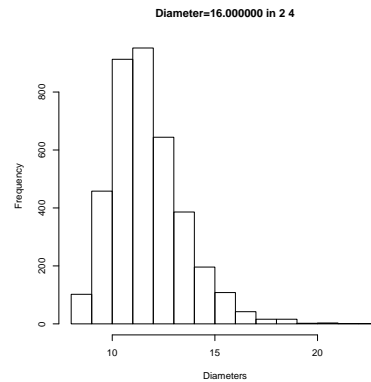


(f) Only edges with tour frequency more than ten

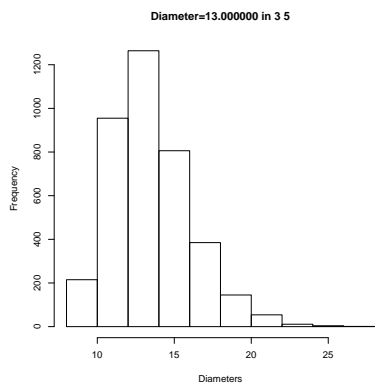
Figure 11: Degree distributions of the graphs, which arise by taking different tour frequencies into account (see individual caption) from simulations for 10th July 2015. Dotted lines show 10% and 90% quantiles of simulations and solid line shows true distributions.



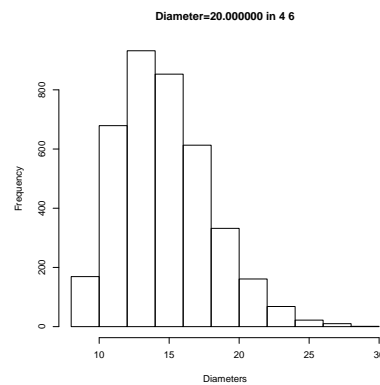
(a) Only edges with four frequency between one to three



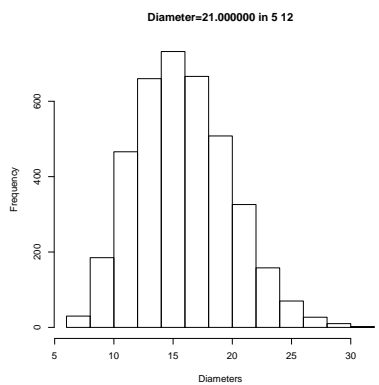
(b) Only edges with four frequency between two to four



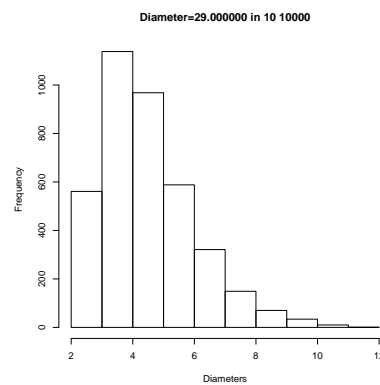
(c) Only edges with four frequency between three to five



(d) Only edges with four frequency between four to six

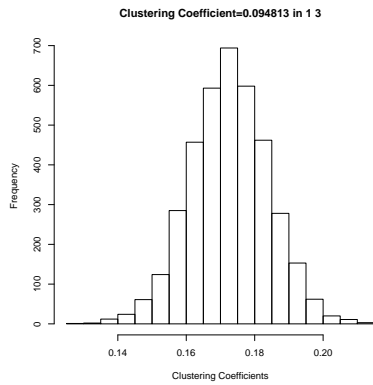


(e) Only edges with four frequency between five to twelve

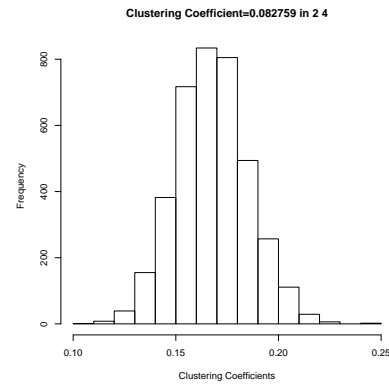


(f) Only edges with four frequency more than ten

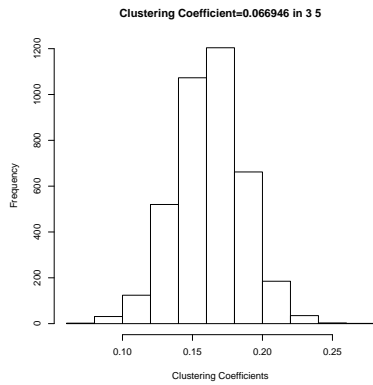
Figure 12: Histograms of diameters of the graphs which arise by taking different edges into account (see individual caption) from simulations for 10th July 2015. In the title of the plot the observed value is shown.



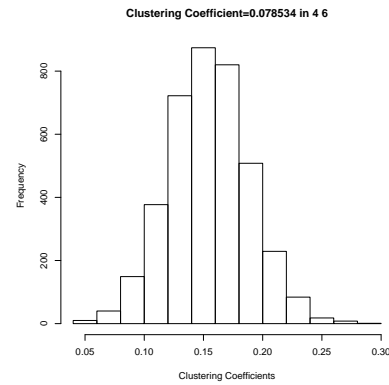
(a) Only edges with four frequency between one to three



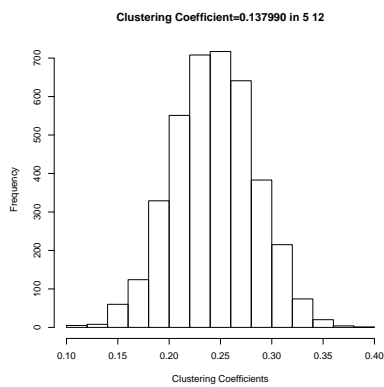
(b) Only edges with four frequency between two to four



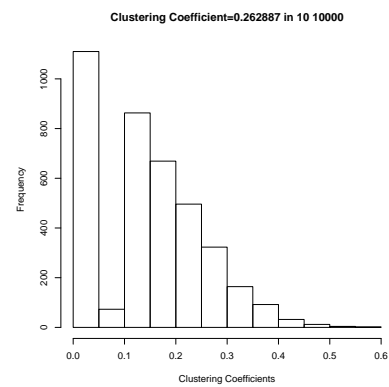
(c) Only edges with four frequency between three to five



(d) Only edges with four frequency between four to six

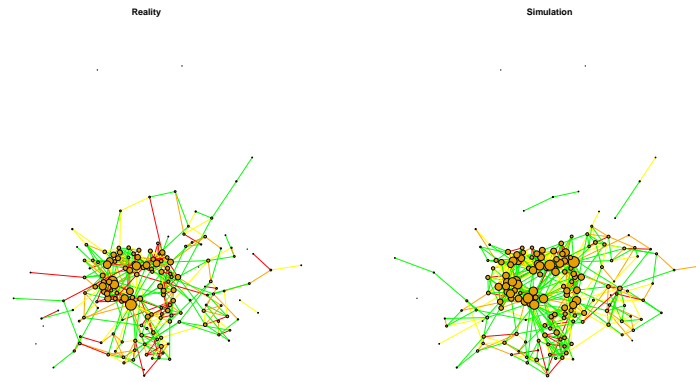


(e) Only edges with four frequency between five to twelve

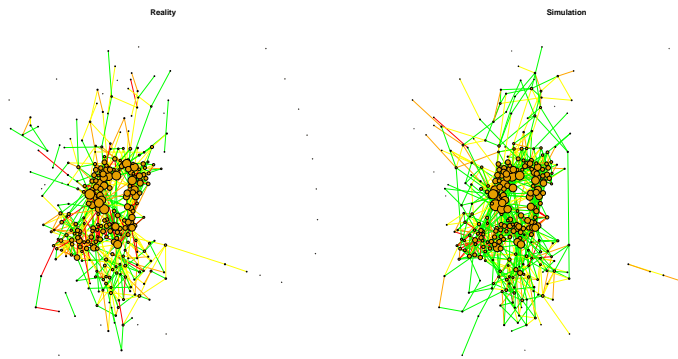


(f) Only edges with four frequency more than ten

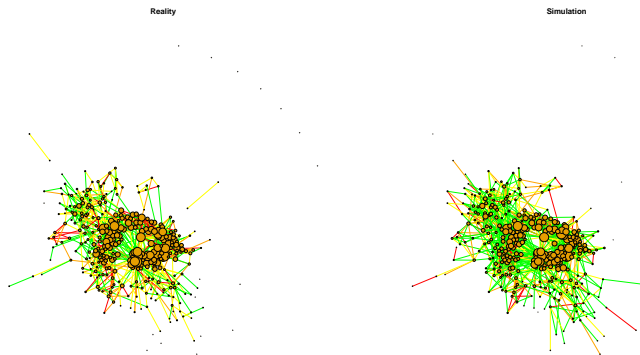
Figure 13: Histograms of clustering coefficients of the graphs which arise by taking different edges into account (see individual caption) from simulations for 10th July 2015. In the title of the plot the observed value is shown.



(a) 12th December 2012



(b) 18th April 2014



(c) 10th July 2015

Figure 14: Compares one simulated graph with the true observation.

squared bias plus variance yields the following asymptotically optimal bandwidths h_K and h_L , minimizing the asymptotic mean squared error:

$$h_K := \left(\frac{1}{l_n} \cdot \frac{\int_{-1}^1 K(u)^2 du}{\left[\int_{-1}^1 K(u)u^2 du \right]^2} \cdot \frac{C_1}{4C_2} \right)^{\frac{1}{5}}.$$

Again, the corresponding expression for h_L can be found by replacing every K by L . So the following formula, known from kernel estimation, holds also true in our setting

$$h_K = \left(\frac{\int_{-1}^1 K(u)^2 du}{\left[\int_{-1}^1 K(u)u^2 du \right]^2} \cdot \frac{\left[\int_{-1}^1 L(u)u^2 du \right]^2}{\int_{-1}^1 L(u)^2 du} \right)^{\frac{1}{5}} h_L. \quad (6.1)$$

This means that knowledge of the bandwidth minimizing the mean squared error for kernel L , implies knowledge of the bandwidth minimizing the mean squared error using kernel K . Ultimately, we use a triangular kernel $K(u) = (1+u)\mathbb{1}_{[-1,0)}(u) + (1-u)\mathbb{1}_{[0,1]}(u)$. In order to find the bandwidth h_K for this kernel, we want to apply cross-validation. As proposed in Hart and Yi (1998) one-sided cross validation is an attractive method for the case of time series data. One-sided here means that we apply cross validation to a kernel L which is only supported on the past $[-1, 0]$. In order to avoid a bias, we use the one-sided kernel together with local linear approximation. This following heuristic derivations motivates this choice.

Firstly, in our regular maximum likelihood setting, we maximize, over $\mu \in \Theta$, the expression

$$\begin{aligned} & \sum_{0 < t \leq T} \frac{1}{h} K\left(\frac{t-t_0}{h}\right) \sum_{(i,j) \in L_n} \Delta N_{n,ij}(t) \mu^T Y_{n,ij}(t) \\ & \quad - \int_0^T \sum_{(i,j) \in L_n} \frac{1}{h} K\left(\frac{t-t_0}{h}\right) C_{n,ij}(t) e^{\mu^T Y_{n,ij}(t)} dt \\ \approx & \sum_{0 < t \leq T} \frac{1}{h} K\left(\frac{t-t_0}{h}\right) \sum_{(i,j) \in L_n} \Delta N_{n,ij}(t) \mu^T Y_{n,ij}(t) \\ & \quad - \int_0^T \sum_{(i,j) \in L_n} \frac{1}{h} K\left(\frac{t-t_0}{h}\right) C_{n,ij}(t) e^{\theta_0(t_0)^T Y(t)} \\ & \quad \times \left(1 + (\mu - \theta_0(t_0))^T Y_{n,ij}(t) + \frac{1}{2} [(\mu - \theta_0(t_0))^T Y_{n,ij}(t)]^2 \right) dt. \end{aligned}$$

Deriving this expression with respect to μ , setting the derivative equal to zero, and rearranging terms, yields (to save space we use here a fraction, although the denominator is a matrix)

$$\hat{\theta}_K(t_0) - \theta_0(t_0)$$

$$\approx \frac{\sum_{(i,j) \in L_n} \frac{1}{h} K\left(\frac{t-t_0}{h}\right) \Delta N_{n,ij}(t) Y_{n,ij}(t) - \int_0^T \frac{1}{h} K\left(\frac{t-t_0}{h}\right) C_{n,ij}(t) Y_{n,ij} e^{\theta_0(t_0)^T Y_{n,ij}(t)} dt}{\sum_{(i,j) \in L_m} \int_0^T \frac{1}{h} K\left(\frac{t-t_0}{h}\right) Y_{n,ij}(t) Y_{n,ij}(t)^T e^{\theta_0(t_0)^T Y_{n,ij}(t)} dt}.$$

Using the notation $y_1 := \mathbb{E}(Y_{n,ij}(t_0) e^{\theta_0(t_0)^T Y_{n,ij}(t_0)} | C_{n,ij}(t_0) = 1) \cdot \mathbb{P}(C_{n,ij}(t_0) = 1)$ and $y_2 := \mathbb{E}(Y_{n,ij}(t_0) Y_{n,ij}(t_0)^T e^{\theta_0(t_0)^T Y_{n,ij}(t_0)} | C_{n,ij}(t_0) = 1) \cdot \mathbb{P}(C_{n,ij}(t_0) = 1)$, we obtain the approximation

$$\hat{\theta}_K(t_0) - \theta_0(t_0) \approx \frac{\sum_{(i,j) \in L_n} \sum_{0 < t \leq T} \frac{1}{h} K\left(\frac{t-t_0}{h}\right) \Delta N_{n,ij}(t) Y_{n,ij}(t) - y_1}{y_2}. \quad (6.2)$$

Now define the local linear estimator $\hat{\theta}_{LC,K}(t_0)$, with respect to a kernel K , as the value of μ_0 maximizing the following expression over $(\mu_0, \mu_1) \in \Theta^2$:

$$\begin{aligned} & \sum_{0 < t \leq T} \frac{1}{h} K\left(\frac{t-t_0}{h}\right) \sum_{(i,j) \in L_n} \Delta N_{n,ij}(t) [\mu_0 + \mu_1(t-t_0)]^T Y_{n,ij}(t) \\ & - \int_0^T \sum_{(i,j) \in L_n} \frac{1}{h} K\left(\frac{t-t_0}{h}\right) e^{[\mu_0 + \mu_1(t-t_0)]^T Y_{n,ij}(t)} dt. \end{aligned}$$

Using the same approximations as in the usual kernel estimation setting, and deriving the resulting approximate likelihood, we obtain

$$\hat{\theta}_{LC,K} - \theta_0(t_0) \approx \frac{\sum_{(i,j) \in L_n} \sum_{0 < t \leq T} \frac{1}{h} K\left(\frac{t-t_0}{h}\right) \frac{M_2 - \frac{t-t_0}{h} M_1}{M_2 - M_1^2} \Delta N_{n,ij}(t) Y_{n,ij}(t) - y_1}{y_2},$$

where $M_k := \int_{-1}^1 u^k K(u) du$. The previous computations were just a heuristic. But nevertheless, the similarity between the previous display and (6.2) suggests that the local linear estimator $\hat{\theta}_{LC,K}$ using the kernel K is actually just a regular kernel estimator $\hat{\theta}_L$ with kernel function

$$L(u) = K(u) \frac{M_2 - u M_1}{M_2 - M_1^2}. \quad (6.3)$$

This aligns with results about kernel estimation, as, for example, stated in Mammen et al. (2011). It can be easily computed that this new kernel is of order one, i.e., $\int u L(u) du = 0$, even though the original kernel was not. Hence, knowledge of the optimal bandwidth for the local linear estimator using the kernel K implies knowledge of the optimal bandwidth for any other order one kernel by means of (6.1). Taking the same route as in Hart and Yi (1998), the selector for the bandwidth \hat{h}_K for the triangular kernel K is the following: Let $K^*(u) := 2K(u) \mathbb{1}_{[-1,0]}(u)$ denote the one sided version of K .

1. Find a bandwidth \hat{h}_L for the local linear estimator $\hat{\theta}_{LC,K^*}$ based on the kernel K^* via cross validation (since we use a one-sided kernel, this step is also called one-sided cross-validation. We will make it more precise later).

2. Compute \hat{h} by using (6.1) with L defined as in (6.3) but with K replaced by K^* .

For the one-sided cross-validation in step 1, we minimize, in our bike share data analysis, the following function in h

$$\frac{1}{k_T} \sum_{k=0}^{k_T} \frac{1}{|L(k)|} \sum_{(i,j) \in L(k)} \frac{\left| e^{\hat{\theta}_{LC,K^*}^{(-k)}(k) T Y_{i,j}(k)} - X_{i,j}(k) \right|^2}{e^{\hat{\theta}_{LC,K^*}^{(-k)}(k) T Y_{i,j}(k)}}, \quad (6.4)$$

where k_T was the number of weeks (recall that we assume the covariates to remain constant over a day, and that we only consider Fridays), i.e., k refers to the k -th Friday in the dataset. $L(k)$ refers to the set of pairs (i, j) between which there was a bike tour on Friday k , $X_{i,j}(k)$ is the true number of bike tours observed between i and j on Friday k . Finally, $\hat{\theta}_{LC,K^*}^{(-k)}(k)$ is the local linear estimator with respect to the kernel K^* based on all but the k -th Friday. Since K^* is left-sided, this really means the estimator is based on Fridays $0, \dots, k-1$, and hence the term one-sided cross-validation. The intensities are the theoretical values of the expectation of the number of bike tours if the model is correct. So we compute the squared difference with the true number of bike rides and divide by the estimated intensity, where we only take the non-censored edges into account.

In Section 3, we had displayed results for different bandwidths h of (6.4) in Figure 5. The prediction error of the fit decreases, until the bandwidth is equal to 23. Afterwards the prediction error stays roughly the same and starts to increase when the bandwidth reaches a full year (52 weeks). This may be explained by a periodicity with a period of approximately one year. If one uses 23 as minimal value we get as asymptotic optimal bandwidth 12 which is approximately 23 divided by ρ . Here, following Step 2 of the above described procedure, we use that ρ is approximately equal to 1.82 for triangular kernels.